2012

FRP stiffener efficiency coefficient for SBS shear strengthening applications

Hamed BabaizadehRoshanfekr
Louisiana State University and Agricultural and Mechanical College, hbabai1@tigers.lsu.edu

FRP STIFFENER EFFICIENCY COEFFICIENT FOR SBS SHEAR STRENGTHENING APPLICATIONS

A Thesis

Submitted to the Graduate Faculty of the
Louisiana State University and
Agricultural and Mechanical College
in partial fulfillment of the
requirements for the degree of
Master of Science

in

Civil and Environmental Engineering

by
Hamed BabaizadehRoshanfekr
B.S., Amirkabir University of Technology 2010
December 2012

To my family specially my beloved father who was always there for me, gave me the best advice, and supported every decision I made in my life.

ACKNOWLEDGEMENTS

I would like to express my truthful gratitude to my advisor Dr. Ayman Okeil for the continuous support of my Master's study and research, for his patience, motivation, enthusiasm, and immense knowledge. His guidance helped me in all the time of research and writing of this thesis. I could not have imagined having a better advisor and mentor for my graduate studies. I would also like to thank my graduate committee members, Dr. Steve Cai and Dr. Suresh Moorthy, for their support, guidance and helpful suggestions. Their guidance has served me well and I owe them my heartfelt appreciation. This research is sponsored in part by the National Science Foundation (CMMI# 1030575). The donation of materials by Fyfe Co., LLC and support from Strongwell are greatly appreciated. Additional support from the Department of Civil and Environmental Engineering at Louisiana State University is also acknowledged. Any opinions, findings, and conclusions or recommendations expressed in this material are those of the authors and do not necessarily reflect the views of the sponsoring agencies.

TABLE OF CONTENTS

LIST OF TABLES

LIST OF FIGURES

ACRONYMS, ABBREVIATIONS, AND SYMBOLS

AASHTO	American Association of State Highway and Transportation Officials
ACI	American Concrete Institute
ASTM	American Society for Testing and Materials
C	shear strength coefficient
CFRP	Carbon Fiber Reinforced Polymer
D	web depth
d_0	stiffener spacing
E	modulus of elasticity
E_{el}, E_{in}, E_{total}	energy (elastic, inelastic, and total)
FE	Finite Element
FRP	Fiber Reinforced Polymer
F_y,F_{yw},F_{yf}	yield stress of steel (general, web, and flange)
GFRP	Glass Fiber Reinforced Polymer
LCC	Life Cycle Cost
LRFD	Load and Resistance Factor Design
LSU	Louisiana State University
r	radius of gyration
RP	rectangular panel
SBS	Strengthening-By-Stiffening
SP	square panel
SS	steel stiffener
t_f	flange thickness
t_w	web thickness
V_n, V_p	shear strength (nominal and plastic)
$V_{NoStiff.}$, V_{SS}, V_{SBS}	shear strength (no FRP stiffener, steel stiffener, Strengthen-By-Stiffening)
V_{val}, V_{exp}	validated shear strength, experimented shear strength
ε_s	strain in steel
λ	slenderness of web
Δ, Δ_{el}	deformation (general and elastic limit)

ABSTRACT

The use of composite materials such as Fiber Reinforced Polymer (FRP) to strengthen concrete structures has surged during the past two decades as an alternative for conventional methods of structural strengthening and repair. FRP materials are light and relatively easy to install. They are noncorrosive, durable and less vulnerable to environmental conditions in comparison to other construction and retrofitting materials. The knowledge and applications of composites for strengthening steel structures are relatively smaller when compared to concrete strengthening applications. Strengthening-By-Stiffening (SBS) is a new strengthening alternative that was developed at Louisiana State University. SBS has proven to be a practical technique for inhibiting local buckling in shear-controlled steel beams. This technique relies on the out-of-plane stiffness of pultruded composite sections as opposed to the in-plane strength of thin composites that is often reported in the literature. Preliminary results showed that gains in shear strength of more than 40% are achievable using SBS.

The objective of this study is to establish a coefficient for the efficiency of FRP stiffeners as compared to steel stiffeners. This coefficient can be multiplied by the capacity of steel stiffened structures to obtain the capacity of an FRP stiffened member using a SBS design approach, which is lacking in the current codes that do not address FRP stiffening. Four steel beams were first experimentally tested to verify the developed analytical model under a single point loading over the first internal stiffener and the results were compared to those obtained from a nonlinear finite element (FE) analysis. The beams were designed to evaluate the effects of bonding area between pultruded Glass Fiber Reinforced Polymer (GRFP) stiffener and the web of steel plate girders in addition to the effect of web slenderness and the aspect ratio of the shear panel.

The results show that there is a good agreement between the FE model and the experimental results. The average estimated strength of the tested beams was about 98% of the experimentally obtained capacities. The parametric studies show that the predicted shear capacity of the SBS beams was almost identical with the shear capacity of steel stiffened beams.

CHAPTER 1: INTRODUCTION

A large number of structural elements in the civil infrastructure are aging and are in need for strengthening or complete replacement. The huge costs to the owners of full replacement render this option prohibitive in many cases. Traditional techniques for strengthening steel structures including welding, bolting or adhesive bonding of steel cover plates to the existing systems are sometimes uneconomical, not feasible, or excessively intrusive. Therefore, developing innovative strengthening techniques for steel structures have surged in recent years. The aforementioned traditional techniques have been extensively used in the field which revealed some of their disadvantages such as (1) sensitivity of the repaired systems to fatigue problems due to stress concentrations caused by welding or bolting techniques, (2) quality of field welding which is sometimes in question, (3) difficulty of handling heavy steel plates during repair and installation, (4) long duration of service interruption in the period of installation and necessity of cumbersome framework, and (5) corrosion vulnerability of steel strengthening elements to the environment. The superior properties of composite materials such as Fiber Reinforced Polymer (FRP) composites have led to an increase in their popularity in structural strengthening applications. FRP materials are light and relatively easy to install. They are noncorrosive, durable and less vulnerable to environmental conditions in comparison to other construction and retrofitting materials. Their strength is extremely high relative to their weight, and they have high resistance to abrasion and fatigue (ACI Committee 440 2002; Alsayed et al. 2000; Moy 2001; Tavakkolizadeh 2003; Teng JG et al. 2002).

The literature shows that most strengthening applications using composite materials have been focused on concrete, masonry and wood structures; while there are fewer studies on their use in steel structures. Furthermore, the majority of the research conducted on composite

materials for strengthening focused on providing additional capacity to tensile regions of deficient structural members. Structural member's flexural capacity improves due to additional tensile resistance caused by externally bonding FRP to the tension side of a cross section under bending moments (Nanni 1993). In addition to flexural capacity increase, shear capacity also increases due to additional tensile resistance provided by an FRP plate placed in a direction to resist the diagonal tension caused by shear forces (Khalifa et al. 1998). Based on all of the tests and research on these materials, the knowledge of the behavior of composite materials in concrete strengthening applications has evolved from a development stage to field applications. As a result, codes and guidelines on how to use FRP materials in concrete structure and the related strengthening techniques have been developed by code committees (ACI Committee 440 1996; ACI Committee 440 2002; CSA 2002; ACI Committee 440 2003).

The mechanical properties of steel compared to concrete are better, e.g., higher yield strength and modulus of elasticity. Therefore, in order to utilize FRP for strengthening of steel structures, a large amount of composite materials is required which makes this strengthening technique less effective for steel structures than for concrete structures when used as a tensile force supplement. Consequently, the knowledge and applications of composites for strengthening steel are less relative to its use in concrete applications. Nevertheless, the availability of high modulus FRP materials has shown great potential for new steel strengthening applications in recent years (Schnerch et al. 2004).

The current study and its precursors investigates a new approach to strengthening of steel structures in which the strength increase achieved by stiffening buckling prone regions using pultruded FRP sections where the tensile capacity of FRP is not a major factor in the strengthening scheme. In other words, higher strength of FRP-stiffened steel structures is

achieved by delaying premature unstable modes of failure. This technique is well-suited for thin-walled steel members where local buckling is a major design issue. This strengthening technique, which is now referred to as Strengthening-By-Stiffening (SBS), has been developed at Louisiana State University (Okeil et al. 2009b).

Figure 1 shows the new SBS technique and the classic steel stiffening. The main difference between the two techniques lies in the way the stiffener is attached to the slender steel plate. Typically, steel stiffeners are welded to the steel plate. Conversely, adhesion bonds the FRP stiffener to the steel plate over the stiffener's wide flange area in SBS.

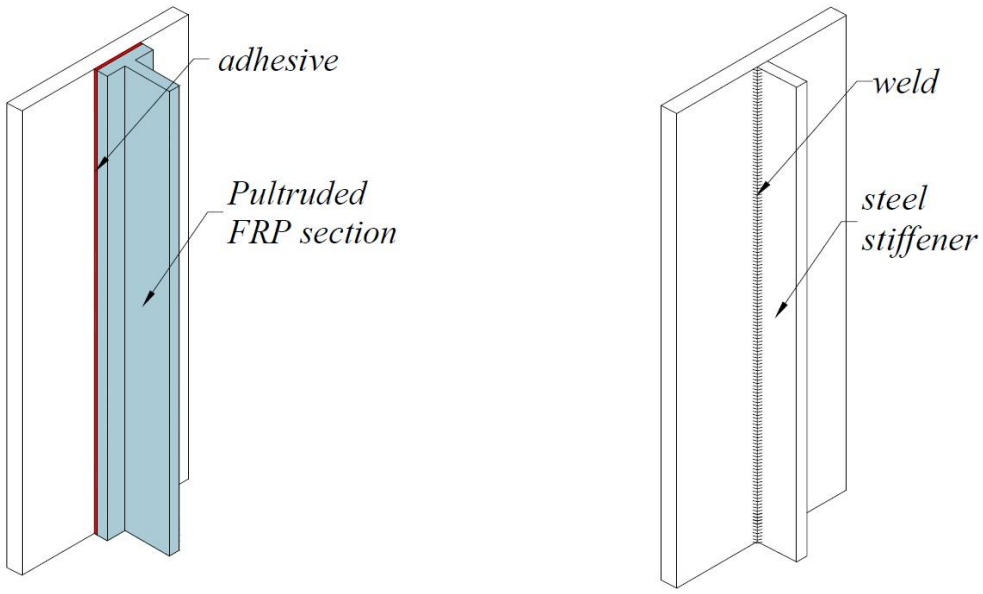

(a) Proposed epoxy-bonded FRP stiffener (b) Conventional welded steel stiffener

Figure 1 – Proposed FRP stiffeners vs. conventional steel stiffeners (Okeil et al. 2009b)

In addition to experimental testing of FRP stiffening, a finite element (FE) model was developed in order to explore the effectiveness of the proposed technique beyond the limitations of laboratory testing. The results of experimental tests and FE analyses are presented and

recommendations for further research are made to suggest a new path in exploring economical FRP strengthening of steel members in constructions.

Additionally, a design coefficient is also established using the relative ratios of shear capacities of the beams with FRP stiffener, steel stiffener, and without stiffener. This ratio expresses the values which should be multiplied by the shear capacity of steel beams with/without steel stiffener to estimate the shear capacity of the similar beam stiffened with FRP. The derived values show a very strong acceptance with the experimental beams tested in the laboratory.

This thesis is organized into 6 chapters. In the introduction of the thesis, chapter 1, the problem is presented and the objectives of the research are introduced. A literature review of related work is summarized in chapter 2. Chapter 3 describes the experimental program designed in order to investigate the objectives. Moreover, it includes the information about the materials, test setup and procedure of the tests. A Finite Element (FE) model is developed in chapter 4 to follow the experimental program. The developed FE model for the introduced stiffening technique includes a parametric study of various parameters which optimizes the technique and finally validates the experimental results. The results of experimental and parametric studies are comprehensively discussed in Chapter 5. Furthermore, Chapter 5 introduces a method to develop an efficiency coefficient for FRP stiffening which is lacking in design code provisions and the efficiency of FRP stiffening is compared to the most common stiffening system, steel stiffening. Conclusions of the results based on experimental and parametric studies are explained in details in chapter 6. Since the Strengthening-By-Stiffening (SBS) is a novel technique, full understanding of it is still a work in progress. Therefore, some recommendations for further work in this field are suggested as well.

CHAPTER 2: LITERATURE REVIEW

A significant amount of research has been published on the use of composite materials to strengthen structural steel members in Europe, Japan, Canada and the Unites States (Nanni 1995; Saadatmanesh and Ehsani 1998; Benmokrane and Rahman 1998; Hassan and Rizkalla 2002). Most of these efforts have focused on the use of Carbon Fiber Reinforced Polymer (CFRP) composites to improve the strength of structural elements by relying on the in-plane properties of thin sheets or plates of the material. However, composite materials are still considered in their youth in comparison to classical alternatives such as steel. Therefore, there are still issues that hinder the full utilization of composite materials in contrast to the classical technologies for strengthening and repair. For example, production of composite material components compared to traditional strengthening alternatives is costly in most cases. The main causes of this cost difference may be limited fabrication of these materials and major equipment related expenses. It is of great importance to focus on utilizing the machinery and devote to expand the fabrication based on market needs, in order to achieve a competitive composites target costs on future commercial structural strengthening. Also, recycling of these materials and other auxiliary components used in strengthening methods such as epoxies may be hazardous to the environment which should be taken into consideration (Stickler 2002). Moreover, at this moment there are no long-term data available to predict the life of FRP strengthening systems and their environmental degradation.

The use of FRP composite materials has become relatively common in infrastructure and structural applications. Majority of existing applications involve FRP strengthening of concrete members or systems. Nevertheless, a relatively small effort is given to FRP strengthening of steel

structural systems. The review of FRP strengthening in this study focuses on stiffening of steel structures rather than concrete.

Regardless of the way FRP is utilized for strengthening steel structures, there are number of identified failure modes. Zhao et al. identified 6 failure modes, which can be seen in Figure 2 (Zhao and Zhang 2007). These failure modes are;

(a) Steel and adhesive interface failure

(b) Cohesive failure (adhesive layer failure)

(c) FRP and Adhesive interface failure

(d) FRP delamination (separation of some carbon fibres from the resin matrix)

(e) FRP rupture

(f) Steel yielding.

2.1 Bonding of FRP Stiffener

Debonding of FRP stiffeners from the steel sections is the most common failure mode in the new strengthening technique, SBS. The stress and bond strength are functions of materials' properties including poisson's ratio, shear and flexural strength, Young's modulus and shear and flexural modulus of the adhesive and Young's modulus of the FRP material, and the dimensions, especially the thickness of the adhesive (Zhao and Zhang 2007).

Therefore, the research on the bonding of FRP to steel substrate will first be reviewed. Different test methods were conducted for the purpose of evaluating the bond between FRP and steel. There are many tests for evaluating the bond between FRP and steel. They can be

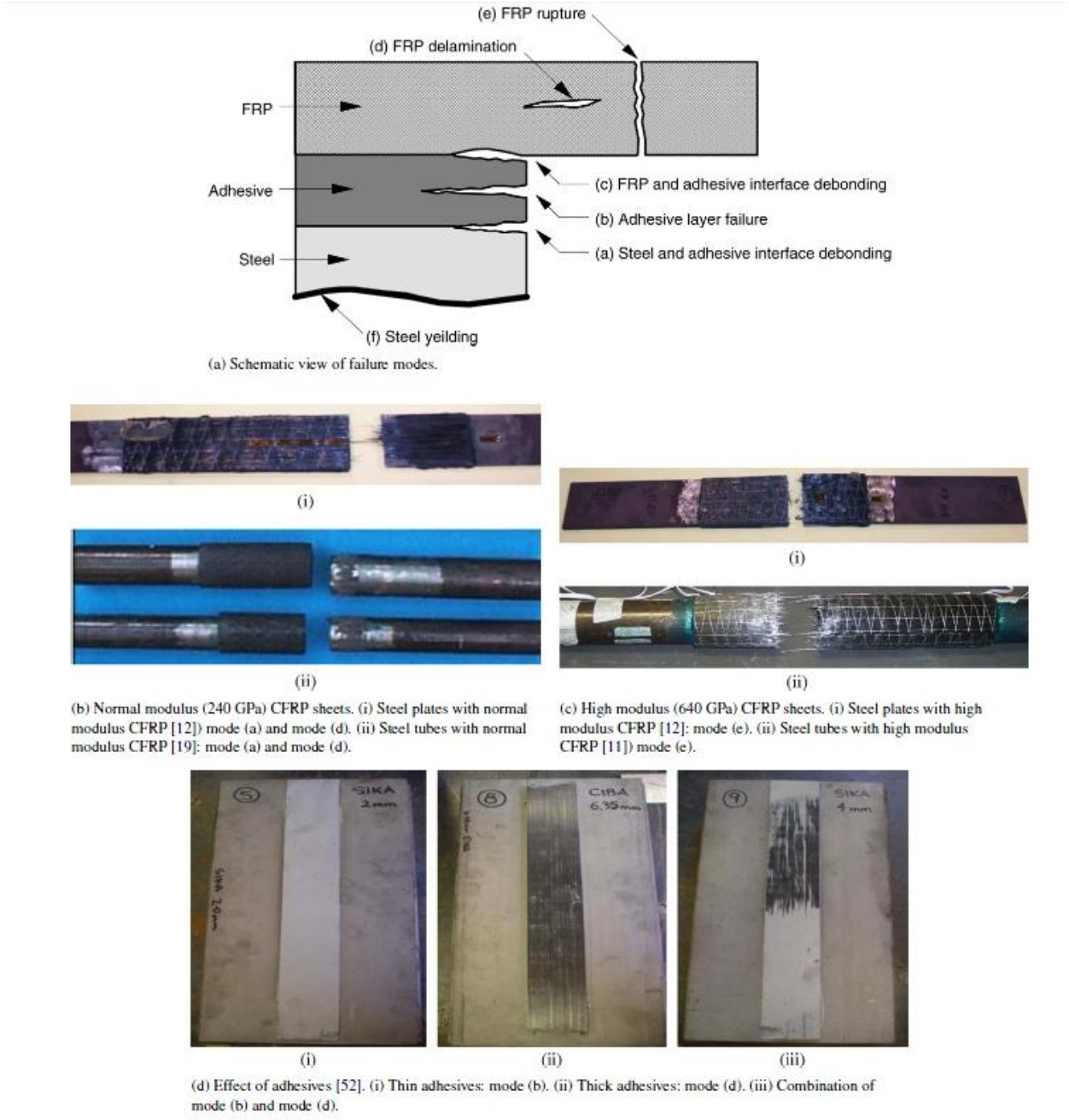

Figure 2 - Failure modes of FRP strengthened steel (Zhao and Zhang 2007)

into 4 main test types (Zhao and Zhang 2007). Figure 3 shows the loading type in Type 1 testing where the steel plate and the FRP are subjected to indirect loads. In this type of testing, a steel plate is bolted to the tension flange of the steel beam and the FRP is attached to the bolted steel plate. A pure bending zone takes place in the beam and the adjacent bolted steel plate and the

attached FRP as a result of the applied flexural loads. Type 1 tests fit bond modeling of I-section beams reinforced by CFRP sections. In Type 2 testing, the steel plate transforms the load directly to FRP as depicted in Figure 4. This type of test is not a very suitable method to test bonding and it is more appropriate for testing of strengthening since if the specimen has a uniform width, yielding of steel may occur outside the FRP strengthened area. In Type 3, as illustrated in Figure 5, the bond strength between CFRP materials and steel plates are assessed by using double strap joints. In this type of test the first thing to consider is predicting the locations in which the debonding will happen. In order to prevent debonding at ends of FRP elements in steel strengthening applications literature suggests techniques such as employing unequal bond lengths, mechanical clapping and transverse CFRP strengthening (Zhao and Zhang 2007; Fawzia et al. 2005). Applying direct compressive or tensile loads to the FRP is the main characteristic of Type 4 tests as shown in Figure 6 which makes it different from the other introduced types of bonding tests. This type is appropriate when the FRP is used in tension rather than compression. One of the considerable drawbacks of applying direct compressive loads to the sections strengthened with FRP is the fact that, in general, FRP materials perform better in tension compared to compression. Therefore, in Type 4 tests there is a strong possibility that the FRP fails itself because of its relatively smaller compression strength. Using CFRP is not highly recommended in type 4 tests since the technique may not be applicable for CFRP sheets because of the difficulty in gripping the sheets (Fawzia et al. 2005).

Lenwari et al. studied the debonding strength of CFRP plates that are adhesively bonded to the bottom flanges of steel beams (Lenwari et al. 2006). They conclude the debonding origins from corner parts of steel and adhesive. They also reported the most important factors influencing stress intensity are thickness of the plate, bond line thickness, plate and adhesive

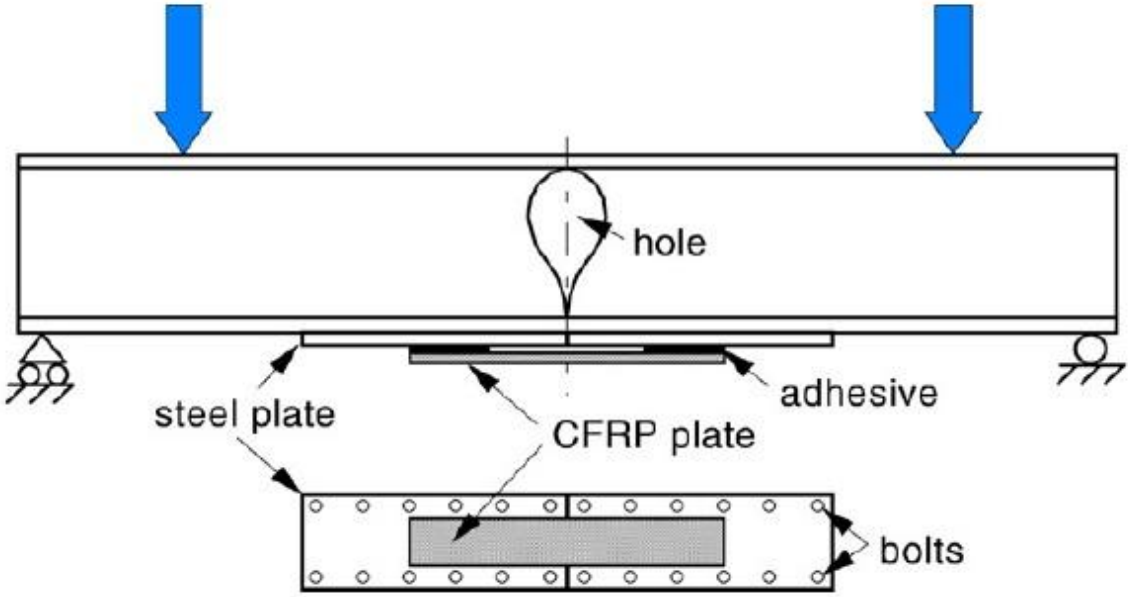

Figure 3- Type 1: Loading is indirectly applied to the FRP and the steel plate in a beam (Zhao and Zhang 2007)

modulus, and spew-fillet angle. The end of the bonded plates is always a dominant debonding region. Also the length of the CFRP does not influence stress intensity significantly. However, spew-fillet conditions may reduce the singularities and stresses near the corner parts where steel and adhesive are connected to each other. Debonding can still occur at other high stress locations such as the ends of the plate where CFRP and the adhesive are joined. Chiew et al. developed a model based on three groups of FRP-steel joints which were tested under static loading (Chiew et al. 2011). The three groups are: (a) double-lap joint (the bond behavior of FRP-steel joint under shear), (b) single-lap joint, and (c) T-peel joint (bond performance under peel dominant condition) as depicted in Figure 7.

It was found that the stress concentration at the ends of the bond is the most important cause of the final bond failure. There is also a critical bond length which produces the maximum bond strength and increasing the length will not increase the strength of the bond. In the tested

FRP stiffened sections the connection between steel and adhesive was the weakest connection in the sections. Consequently, the failure of adhesive was the final failure mode of joints in all different cases. In order to investigate the transmission from steel to the FRP, geometry discontinuity was designed at the end of bond-line and the outcome of the discontinuity was just and only large deformations. The high concentration of stress at the end of the bond-line resulted in bond failure. It was also stated for double lap joints, the maximum shear stress was enormously higher than normal stress while for T-peel joint the maximum normal stress was higher than shear stress. It is worthy to mention for single-lap joint both shear and normal stresses were significantly high (Chiew et al. 2011).

2.2 Flexural Strengthening of Steel Beams

Shaat et al. reported that so far there are four general approaches being used in order to investigate effectiveness and feasibility of strengthening of steel girders (Shaat et al. 2004); (1) Repair of steel girders deteriorate during long time service periods, (2) Repair of purposely notched girder in order to imitate corrosion section loss or cracks due to fatigue, (3) Strengthening of an undamaged section to increase the flexural strength and stiffness, and (4) Retrofit of steel girders in composite action with a concrete deck. Among above introduced cases, last three cases are directly or indirectly related to flexural strengthening as described as follows;

Repair of Notched Girders: Liu et al. developed three-point bending sets of tests using four steel girders. The four W12 x 14 girders were simply supported and the span length of each girder was designed to be 2438 mm. (Liu et al. 2001). The control specimen was the first girder

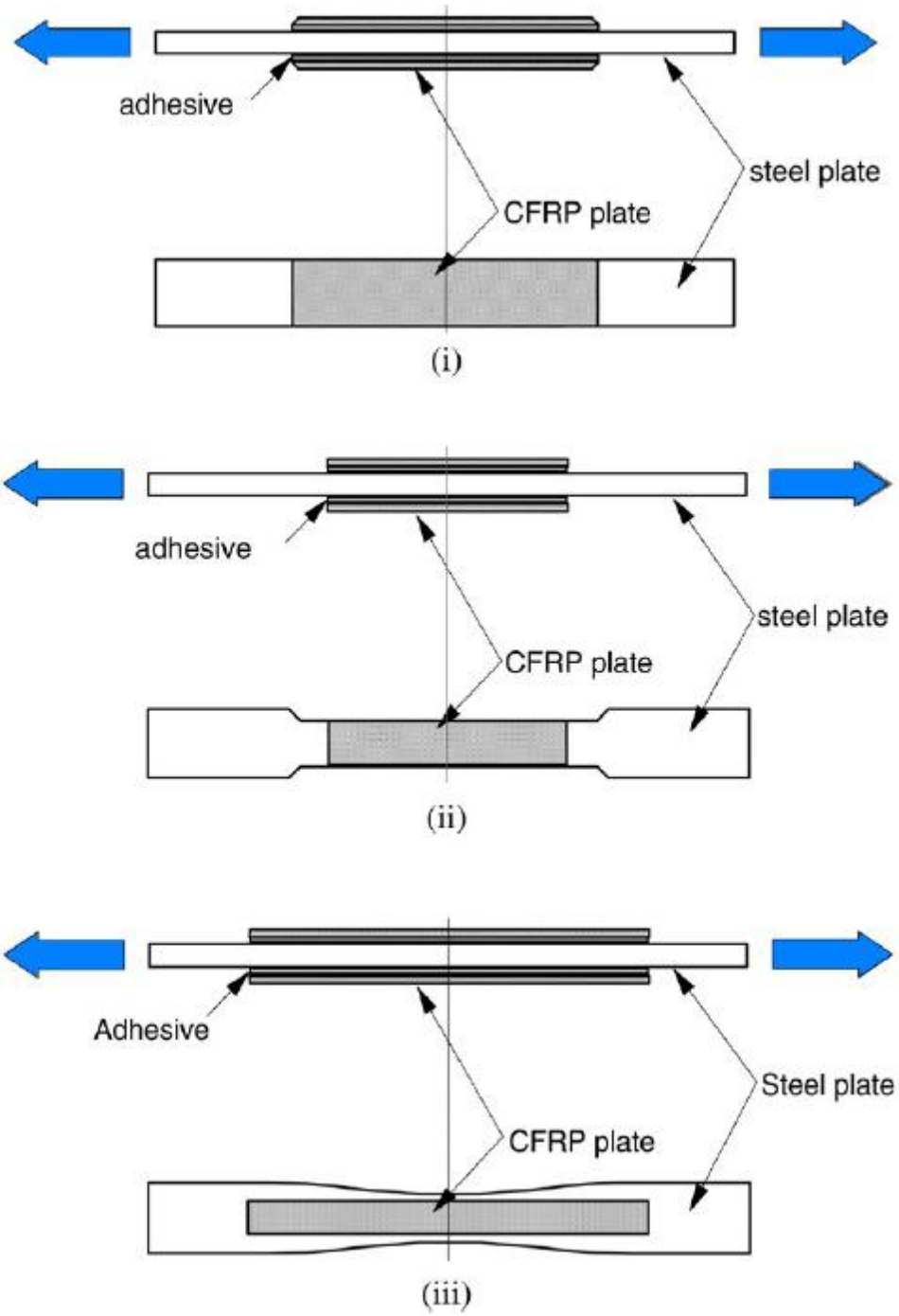

Figure 4- Type 2: Loading is directly applied to the steel element without any gap. (i) Uniform width. (ii) Coupon shape. (iii) Dogbone shape (Zhao and Zhang 2007)

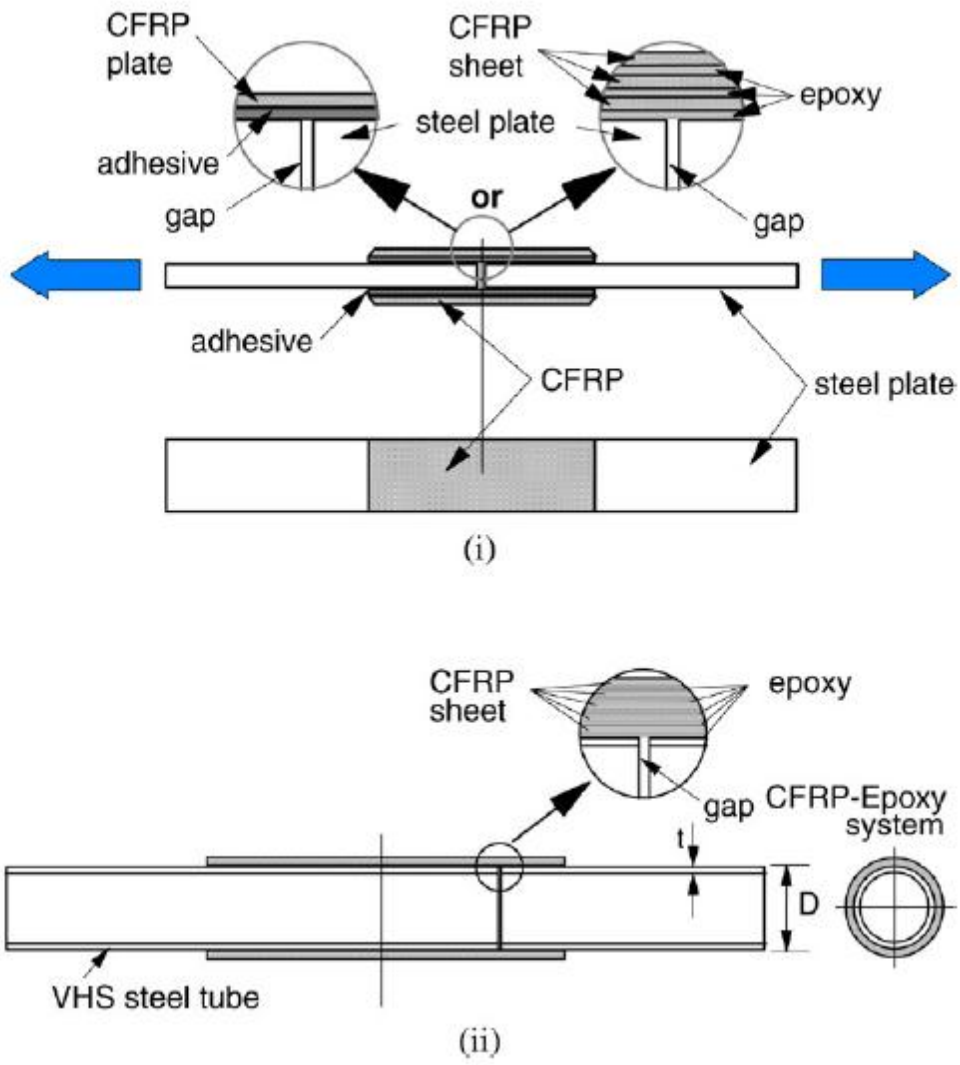

Figure 5- Type 3: Loading is directly applied to the steel element with a gap. (i) Double strap joints. (ii) Single lap joint with circular hollow section (Zhao and Zhang 2007)

which was tested without any type of retrofitting. In order to model a harsh loss of section due to corrosion, the second girder was tested with a 106 mm wide notch on the tension flange without FRP strengthening. In order to examine the effect of the bond length, the rest of the girders were also notched similar to the second girder on the tension flange but the third and the fourth beams were stiffened with 100 mm wide CFRP laminates covering the full length of the beam and one quarter of the beam length, respectively. To decrease the effect of lateral-torsional buckling, four

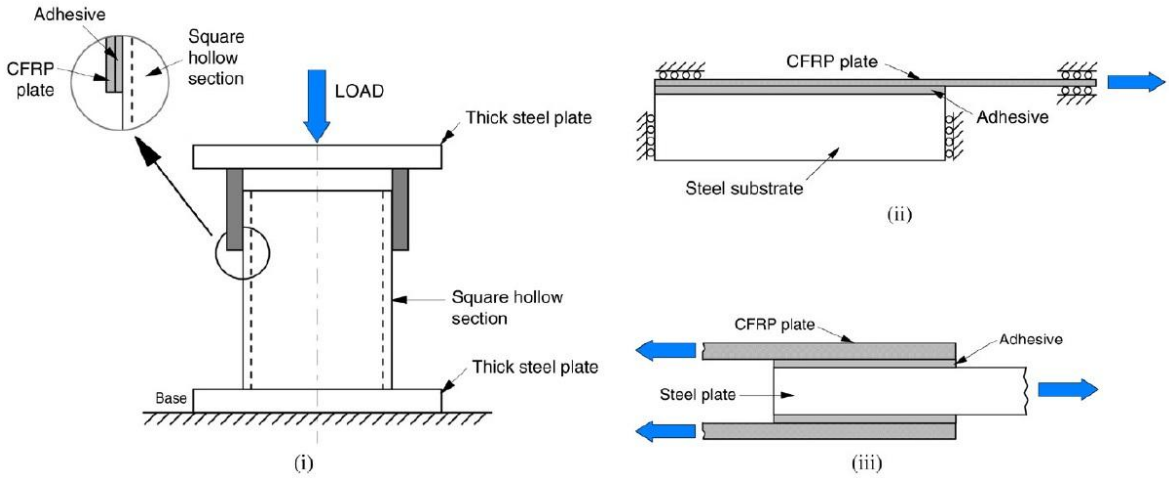

Figure 6- Type 4: Loading is directly applied to the FRP. (i) Shear lap tests. (ii) Single lap shear joint. (iii) Double lap shear joint (Zhao and Zhang 2007)

pairs of lateral supports were located at the support locations and the quarter-span locations.

Lateral buckling was the failure mode for Specimens 1 and 2. On the other hand, the specimen with CFRP laminates on the entire length, specimen 3, failed due to CFRP laminate debonding. The origin of debonding was reported to be at the notch, located at the mid-span of the girder. Then, by increasing the applied load, the debonding propagated to the end of the CFRP laminate. At last, sudden debonding of the CFRP laminate on the fourth specimen was reported as the failure mode. Based on the test results, it was declared that the plastic load capacities of specimens 3 and 4 enhanced 60 and 45 percent, respectively, due to the designed CFRP strengthening.

Strengthening of Undamaged Girders: In another set of experiments, Abushaggur et al. studied the effect of bonding between 19 mm GFRP plates and a W6x25 steel cross section on

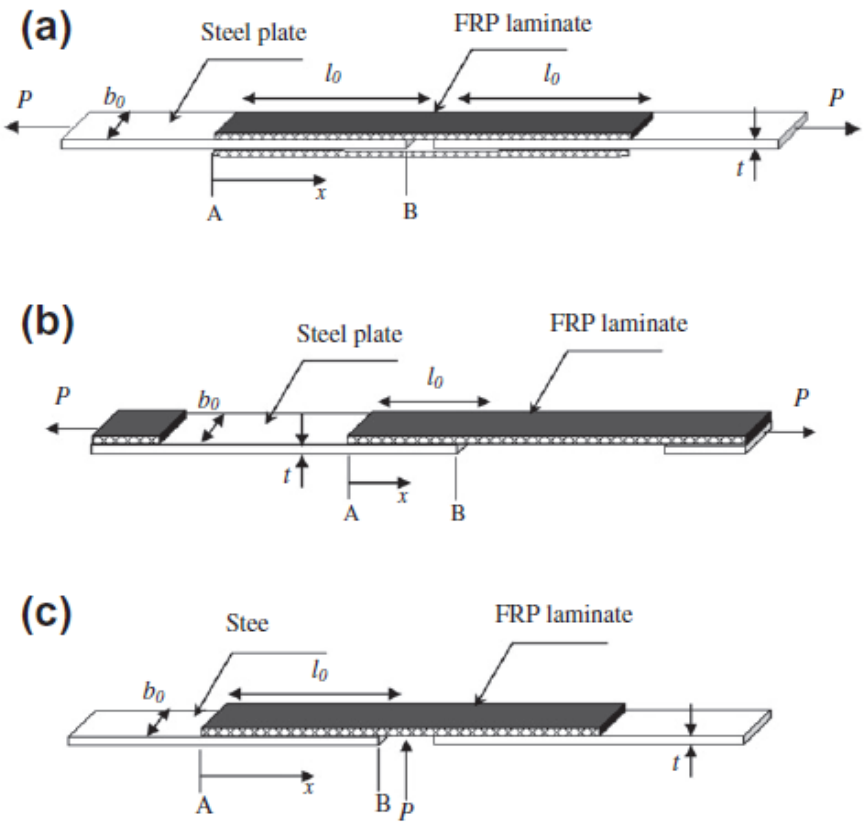

Figure 7- Configurations of (a) double-lap joint, (b) single-lap joint and (c) T-peel joint (Chiew et al. 2011)

capacity increase of the composite section (Abushaggur and El Damatty 2003). Beams of 2800 mm span were subjected to Four-point bending tests, while GFRP plates of 2400 mm length were bonded to both the top and bottom flanges. They reported modes of failure in different cases were either delamination between GFRP layers or rupture of GFRP plates. However, they never reported failure of the adhesive between steel and GFRP as the mode of failure in those set of experiments.

Retrofit of steel girders in composite action with a concrete deck: Tavakkolizadeh et al. performed a comprehensive experimental and analytical study on composite girders (Tavakkolizadeh and Saadatmanesh 2003). Three composite girders were used in the investigation including W14 x 30 steel beams with yield strength 355 MPa, and a 75 mm thick

and 910 mm wide concrete slab attached to the upper steel flange. Two sets of 1, 3, and 5 layers of 75 mm wide and 1.27 mm thick CFRP sheets were attached side by side to the girders. Then, the specimens were tested under a four-point bending test on the 4780 mm long specimens.

Figure 8 shows the behavior of one of the retrofitted girders compared to the behavior of the control (non-strengthened) girder. The results indicate that a significant increase of the ultimate load-carrying capacity of the girders was accomplished. The increase in the beam capacities was reported 44, 51, and 76 percent for the beams retrofitted with 1, 3, and 5 layers of sheets, respectively. The modes of failure for the beams were reported to be concrete slab crushing (for 1 layer of CFRP laminate), debonding of FRP (for 3 layers of CFRP laminates), and concrete slab crushing combined with failure in the web (for 5 layers of CFRP laminates).

Based on the reviewed studies by Shaat et al. (2004), test results of different cases are plotted in Figure 9 to illustrate the effect of CFRP reinforcement ratio on the flexural strength gain for beams with different yield strengths. The reinforcement ratio is defined as the ratio of the area of CFRP to that of the steel section and accounts for the number of the CFRP layers. The presented figure shows the increase in flexural strength as the reinforcement ratio is increased. Additionally, for steel with lower yield strength, the flexural strength increase is higher. Also, the strengthening effectiveness is reduced for thicker laminates as the failure is dominated more by debonding and less by FRP.

2.3 Use of Composites for Inhibiting Local and Global Buckling

The use of composite materials to delay or prevent local buckling in steel flexural members has been the subject of recent investigations. In an analytical study by Sayed-Ahmad the effectiveness of bonding longitudinal CFRP strips along the web of steel beam near and

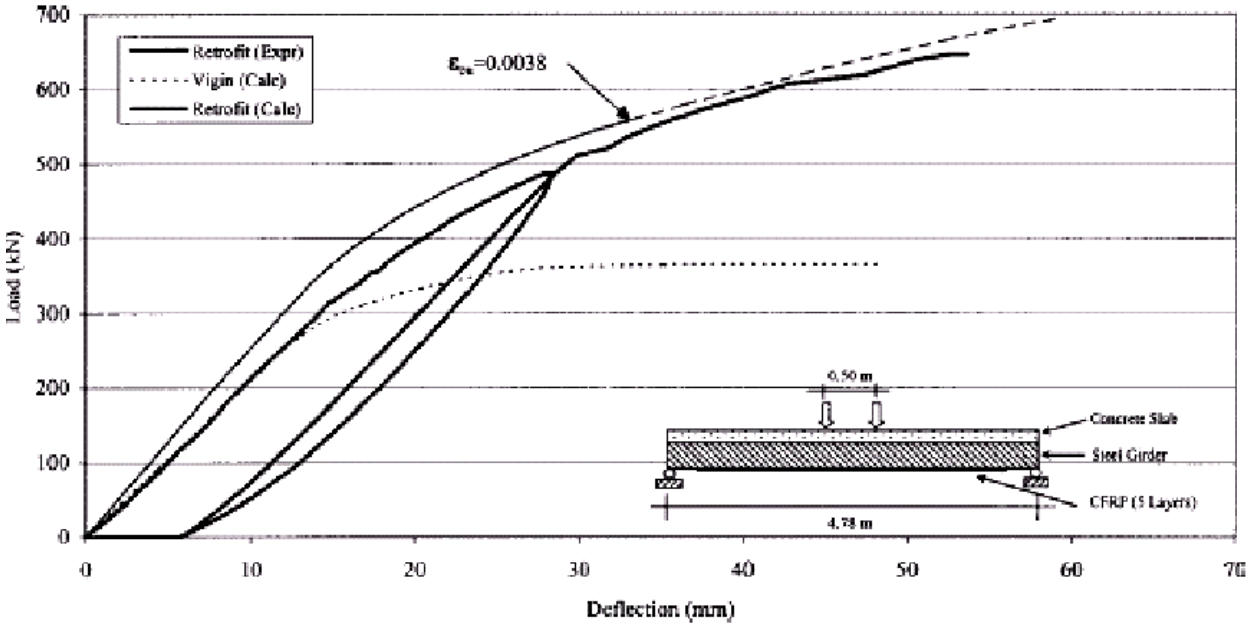

Figure 8- Load-deflection behavior of girder retrofitted with five layers of CFRP sheet (Tavakkolizadeh and Saadatmanesh 2003)

above the neutral axis was investigated (Sayed-Ahmed 2004). Figure 10 shows the different CFRP strengthening configurations considered in the non-linear finite element (FE) analysis, where bending was produced by applying point loads at third points along the beam. Adhesive debonding was not considered in the FE model.

Non-linear finite element modeling was performed to determine the effect of bonding longitudinal strips of low modulus GFRP strips to the compression flange of an I-shaped member by Accord et al. (2006). According to the results of this analysis, addition of the GFRP strips could be effective in increasing the ductility of the member during plastic hinging. Similar to the work by Seyed-Ahmed debonding of the adhesive was not accounted for in the modeling (Sayed-Ahmed 2004).

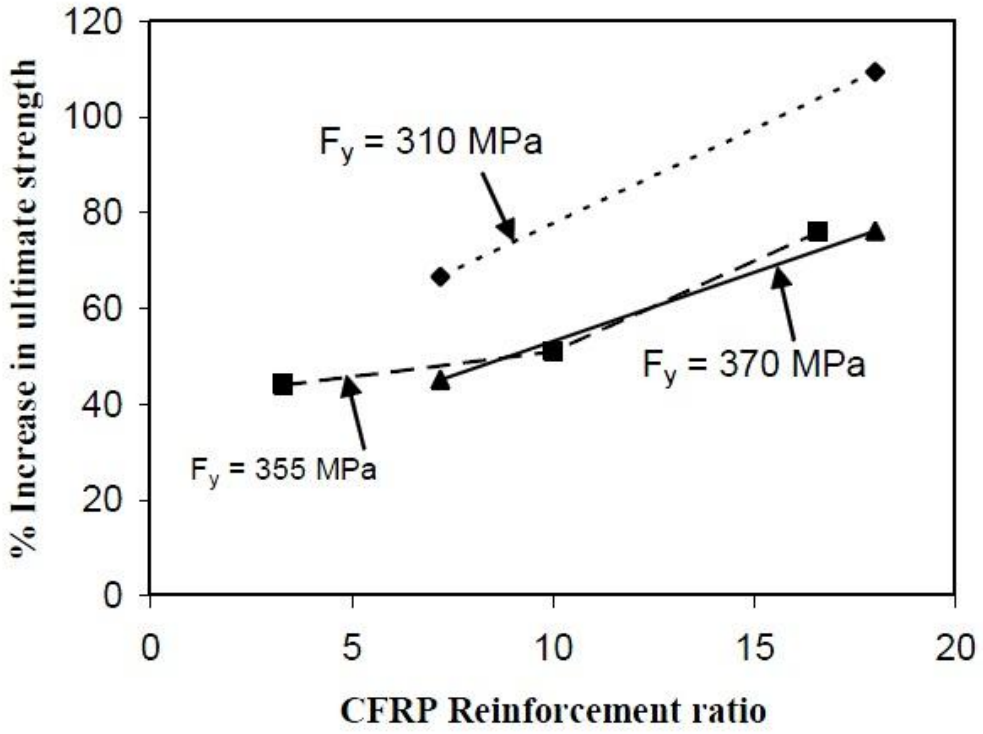

Figure 9- Effect of CFRP reinforcement ratio and yield strength on the ultimate strength of retrofitted steel girders (Shaat et al. 2004)

Harries et al. studied WT shapes subjected to axial force in which the WT shapes were restrained against buckling (Harries et al. 2009). The investigation involved two sets of experiments based on the main goals; (1) study FRP strengthening of the elastic flange tortional buckling (FTB) of slender WT braced subjected to cyclic compression, and (2) study inelastic local buckling of the stem of WT sections. Based on the results of the first set of experiments, it was concluded that FRP strengthening of the WT shapes was not very effective. However, a 46% increase in the load required to cause weak-axis deflection was observed. The outcome of the second set of experiments was a 14% increase in the axial load carrying capacity of the strengthened specimens compared with the control specimen. In the second sets of tests, the weak-axis radius of gyration, r_y, was given attention to those specimens with inelastic buckling

which consequently magnifies the local contribution of the FRP. The radius of gyration increased considerably from 12% to 35% only for WT stem whereas the increase in r_y for the entire shape was not considerable. Other than the elastic buckling specimens failing in FTB which never experienced capacity enhancement because of their r_y nature, the rest of the section properties of the step experienced increase in load carrying capacity.

The behavior of simple span, 11ft. long, TS6×6×3/16 grade A500 steel tubes under different CFRP strengthening configurations was studied by Vatovec et al. (2002). The strengthening materials used in the steel tubes reinforcement were 50 mm × 1.2 m Sika Carbodur™ S512 CFRP strips and SikaDur 30 epoxy adhesive. Some of the specimens had to be filled middle half of their length with normal-weight concrete in order to prevent the possible local buckling. The loading pattern was using of two point loads having the equal distance from the mid-span. The specimens with no concrete filling prone to local buckling were chosen to be the controlled samples. It was observed that the increase in number of CFRP strips results in increase in the strength of the specimens. The failure mode of the strengthened specimens with infill of concrete was reported to be top CFRP strip debonding which happened before delamination of bottom CFRP strips. It was also reported the additional flexural capacity provided by CFRP strips to the steel tubes is limited by local modes failure and also CFRP delamination.

It is clear from recent studies published in the last few years on FRP strengthening of steel structures that improving local and global instabilities is gaining attention of many researchers. The available knowledge in the literature, which is mostly based on experimental testing rather than analytical studies, shows that adhesive debonding is the controlling mode of failure in FRP strengthening of steel members.

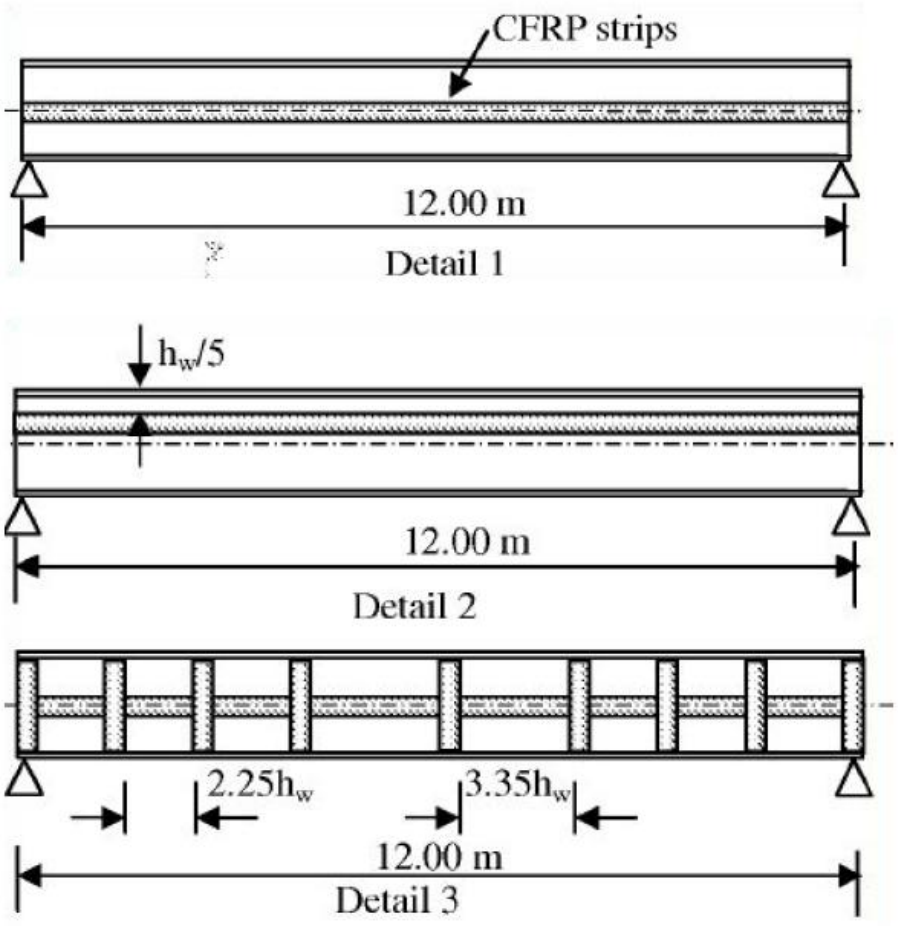

Figure 10– Details of CFRP web strengthening (Sayed-Ahmed 2004)

Several other researchers also investigated the use of FRP composites for inhibiting local and global buckling in different type of steel structures. For example, Zhao and Al-Mahaidi (2009) also investigated to efficiency of CFRP strengthening of light gauge steel beams. They tested different steel webs strengthened with CFRP strips on the inner, outer and both sides of the steel webs to investigate the effectiveness of different conditions of CFRP placing on delaying of web-crippling buckling failure of the specimens. It was concluded that using CFRP strips can substantially enhance the web buckling capacity of steel beams especially for those with higher ratios of web depth to web thickness. Moreover, in other research investigations Shaat and Fam (2006) studied the behavior of short and long square hollow structural section

(HSS) columns strengthened with CFRP sheet under axial loading. They concluded using CFRP sheets can increase the capacity of short and long columns up to 18% and 23%, respectively. Also, El-Tawil and Ekiz (2009) studied the buckling behavior of steel braces strengthened with mortar block cores and FRP wraps.

2.4 Strengthening-By-Stiffening (SBS)

In recent years, the availability of high modulus FRP materials has opened novel paths for new and innovative steel strengthening applications. One of the most recent of these pioneering applications is Strengthening-By-Stiffening (SBS); which was developed at Louisiana State University. It has proven to be a practical method for inhibiting local buckling in shear-controlled steel beams. Preliminary results showed that gains in shear strength of more than 40% are achievable using SBS. This technique relies on the out-of-plane stiffness of pultruded composite sections as opposed to the in-plane strength of thin composites that is often reported in the literature (Okeil et al. 2009b; Okeil 2010; Okeil et al. 2010; Okeil and Broussard 2012; Okeil et al. 2012)

Based on the previous literature review, it can be stated that FRP strengthening of steel structures has mainly focused on in-plane contributions of composite plates, strips, and sheets. This study explores a different approach where low-modulus pultruded GFRP sections are used to improve the out-of-plane stiffness of buckling prone steel members while in most cases CFRP is the material of choice to improve the effectiveness of the strengthening system. The initialization of this approach can be found in the research carried by Okeil et al. (2009a). The idea was initiated by an experimental investigation where beam specimens controlled by out-of-plane web buckling due to shear forces were tested to determine the effectiveness and viability of the proposed strengthening technique.

Identical beams in material properties and geometry were tested to failure taking the same loading pattern with/without stiffening. The stiffeners are pultruded T-shaped GFRP bonded to each side of the failure prone end web panel as described in the next chapter. It was concluded that a 56% higher load was required to induce failure in the GFRP stiffened beam compared to the unstiffened specimen. Using code equations and by treating the GFRP stiffener as steel stiffener, a theoretical determination of its effect on the loaded test was attempted. The code predicted capacity was inaccurate. This may be due to the fact that epoxy debonding is not accounted for in the code. Furthermore, code predictions ignore vierendeel or sway from action which is large for the overdesigned specimens. It was noted that the observations in the experiment indicate that the proposed strengthening technique would be applicable for any structural element prone to local buckling. Further testing of other parameters was needed to fully understand SBS.

CHAPTER 3: EXPERIMENTAL PROGRAM

An experimental program was developed to investigate the effect of two parameters on the efficiency of the SBS technique. Considering all possible modes of failure of unstrengthened section of steel beam including flexure, local flange buckling, steel stiffener buckling, welding, load bearing, and web buckling, the former one; web buckling, was chosen as target mode of failure by overdesigning the beam with respect to the other modes (Okeil et al. 2009a). In fact, considering web buckling failure mode is the best way to achieve the objective of studying which is quantifying the efficiency of using low modulus FRP sections to stiffen buckling prone regions of thin-walled steel structures.

Four steel beam specimens categorized in two groups were tested. The first two specimens (Group A) were designed to study the effect of the bond area on the effectiveness of the SBS technique. The other two specimens (Group B) focused on the web slenderness effect. The specimen dimensions were similar to the specimens previously tested at LSU (Okeil et al. 2009a). As can be seen from Figure 11and Figure 12, Group A specimens had square shear panels (SP) while rectangular shear panels (RP) were used for Group B specimens. This choice complements earlier work where SP and RP specimens were tested, albeit with different bond area and different slenderness for the SP and RP cases, respectively. All SBS specimens had two stiffeners bonded to the critical shear panel.

Each beam was given a designation based on its panel geometry, SP or RP, its web thickness, T1 or T2, and its bond area A1 or A2. For example, specimen SP-wFRP-T1-A1 is a square panel specimen with SBS strengthening, first slenderness group and first bond area. The load was applied using an MTS machine with a capacity of 2500 kN. The load was applied at the first steel stiffener to produce a condition where the test region panel is susceptible to buckling.

The tests were displacement controlled, and the beam was monotonically loaded up to failure. The failure load of the FRP stiffened beams was recorded and compared with the results of the control beams without any stiffeners. The enhancement in shear capacity is assessed from the

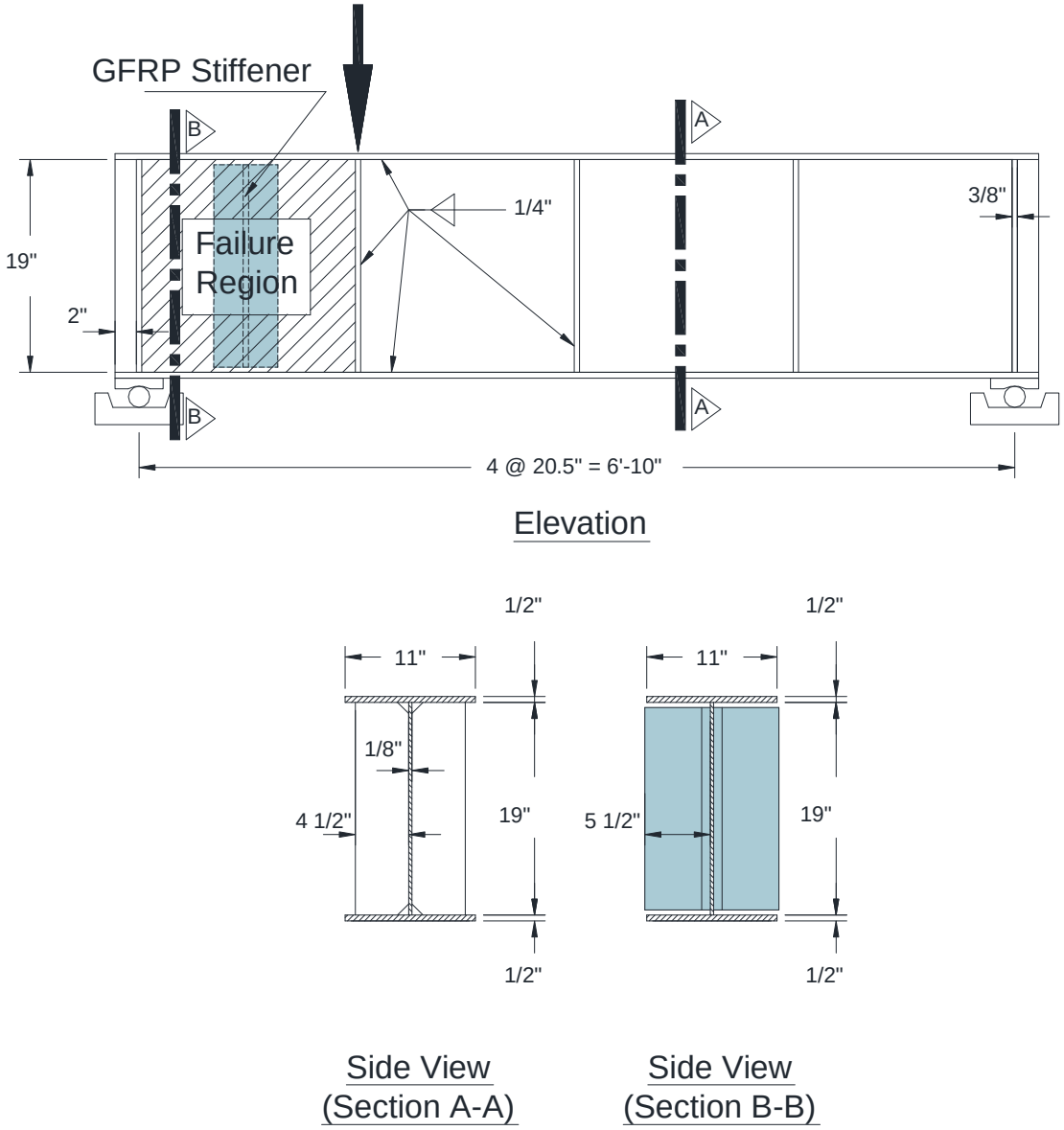

Figure 11- Dimensions of beam specimen in Group A

results of the beams with SBS strengthening results database maintained at LSU. Table 1 lists the details of four specimens.

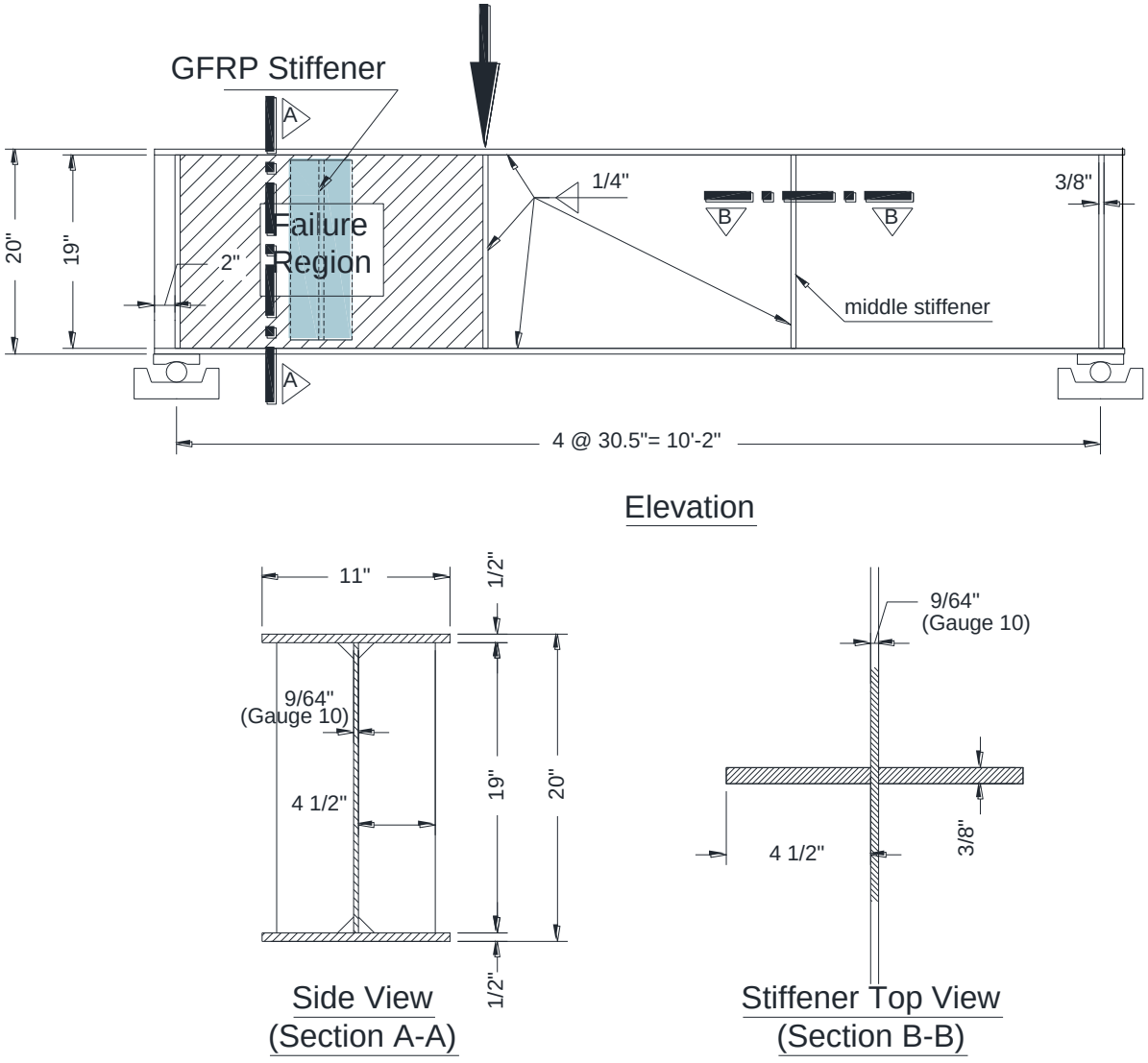

Figure 12- Dimensions of beam specimen in Group B

Table 1– Details of the beams

Specimen	Group	Web Thickness (Nominal [Actual])	Stiffener Flange Width
SP-NoFRP-T1	Group A	0.125” [0.11542"]	-
SP-wFRP-T1-A1	Group A	0.125” [0.11542"]	3"
RP-NoFRP-T2	Group B	0.141” [0.12906"]	-
RPwFRP-T2-A2	Group B	0.141” [0.12906"]	6"

The dimensions of two groups of beams used in this study are shown in the Figure 11 and Figure 12. The width of the stiffener in Groups A and B was 3 in. and 6 in., respectively. The vertical orientation was preferred over diagonal compression strut orientation to avoid applying a large compression force on the stiffener, since that force may cause a premature failure in the stiffener (Okeil et al. 2009a).

3.1 Material Properties

All tested beams were fabricated using A36 steel. The stress-strain relationship of the beams’ steel was obtained from standard coupons that were cut from the same web plate. A MTS 810 Materials Testing System (Capacity 55 kips) equipped with MTS Hydraulic grips and controlled by an MTS TestStar IIs Controller was used for the coupon tests following ASTM E8 (2008). Strains were measured using an MTS extensometer with a gauge length equal to 1 inch. The test setup can be seen in Figure 13 - Coupons test setup.

Wide-flange beams EXTREN® Series 500 6 in. x 3/8 in. Strongwell Glass Fiber Reinforced Polymers (GFRP) pultruded sections were used for stiffening of the specimens. Table 2 lists the basic material properties of the GFRP sections.

a- Testing instrument b-Standard coupons

Figure 13 - Coupons test setup

Table 2 - Mechanical properties of GFRP pultruded longitudinal section*

Property	Value
Tensile Stress, MPa [ksi]	138 [20]
Flexural Stress MPa [ksi]	207 [30]
Modulus of Elasticity MPa [ksi]	17,200 [2,500]

* As provided by the manufacturer (Strongwell Corporation 2008)

It should be noted that the longitudinal modulus of elasticity of the EXTERN product line is 2,500 ksi, which is substantially lower than that of steel. As mentioned earlier, the motivation behind this study was to study the feasibility of using low modulus FRP in strengthening steel structures. It will be shown later that the proposed strengthening technique can still be effective even with low modulus FRP materials. The epoxy used to bond the GFRP stiffeners to the steel specimens is a two-component epoxy (Tyfo S®) manufactured by Fyfe Co.. The epoxy is intended for use with fiber wrap systems. However, it was shown to be effective in earlier SBS tests and its use is continued for the current tests. Table 3 lists the mechanical properties of the used epoxy.

Table 3 - Mechanical properties of epoxy*

Property	Value
Tensile Stress, MPa [ksi]	50 [7.25]
Tensile Modulus, MPa [ksi]	3,180 [461]
Flexural Stress MPa [ksi]	123 [17.90]
Flexural Modulus MPa [ksi]	3,120 [452]
Elongation [%]	5.0

* As provided by the manufacturer (Fyfe Co. 2008)

It is worthy to note that there are other superior epoxies which may be better suited for steel applications; however, this epoxy was chosen for the study to demonstrate that even regular epoxies can be used in the proposed strengthening technique and produce good results.

3.2 Specimen Preparation

The wide flange GFRP beams were cut into T-shaped sections with flange widths of 3 in. and 6 in. for the SP-wFRP-T1-A1 and RP-wFRP-T2-A2 specimens, respectively. A table saw was used to cut the as-delivered EXTERN I-section (see Figure 14) to achieve the desired dimensions of the GFRP stiffeners bonded to the steel beam after removing the glazed finish of

Figure 14– GFRP material used in the study

the original product. Bond surfaces were prepared to enhance epoxy adhesion. The web panel where the GFRP were to be attached was sanded using a drill equipped with sanding rolls and

coarse sandpaper to remove all rust and reach the white metal as shown in Figure 15-a. To enhance the bond between the GFRP and the epoxy, random scratches were made to the surface of the GFRP flange to be bonded to the steel beam after removing the glazed finish of the original product. Figure 15-b shows the FRP stiffener right before bonding to the steel beam. Acetone was then used to clean the surfaces of the flange of FRP and targeted panel of the beam in order to remove the dust and any residual particles to achieve a better bond surface with minimal flaws. Figure 15-b shows the FRP stiffener right before bonding to the steel beam. Acetone was then used to clean the surfaces of the flange of FRP and targeted panel of the beam in order to remove the dust and any residual particles to achieve a better bond surface with minimal flaws.

a- Sanding the steel section to reveal white steel

b- Clean surfaces and making scratches

Figure 15– Stiffener preparation

Finally, epoxy was applied to both surfaces; i.e., of the beam's web and the stiffener's flange, before positioning the stiffener vertically in the middle of the panel as can be seen in

Figure 16. No extra pressure was applied while positioning the epoxied stiffener to the steel beam. Only minor lateral movements were repeated a few times to ensure that the epoxy has covered both bond surfaces. Any extra epoxy that came out from the connecting surface of the stiffener was removed using a putty knife.

3.3 Test Setup and Procedure

The loading setup for beam tests can be seen in Figure 16. A displacement controlled procedure was used to monotonically load the specimens. Loading was stopped at frequent intervals to inspect the specimen and loading setup. Force, deformation and strain readings were recorded at 0.10 sec. intervals. The test was stopped when the applied load dropped 65% of its peak value or a clear yield plateau was observed. This corresponded to a deformation between 0.3 and 0.4 in.

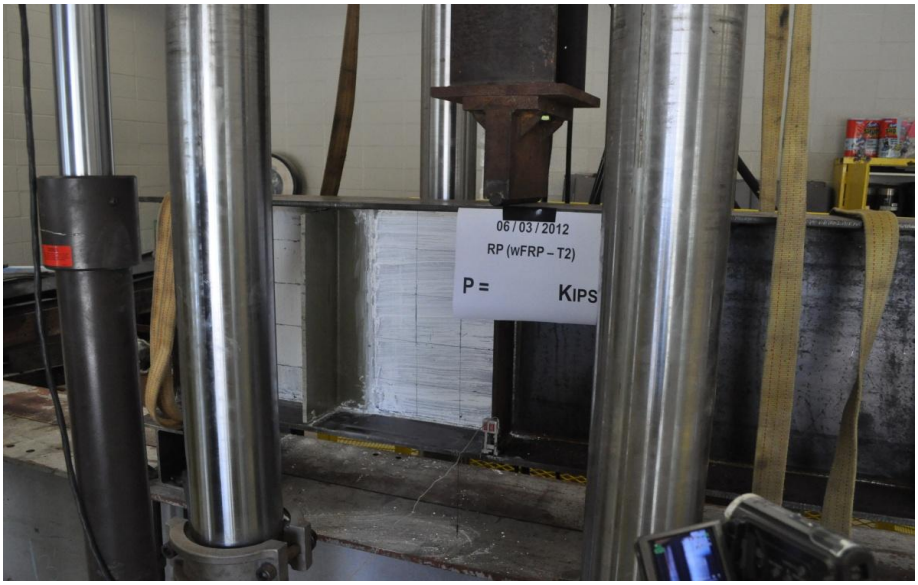

Figure 16– Beam test set up

3.4 Experimental Results

The load-displacement curves for the four tested beams were plotted for each group separately. Two plots are shown in each figure for the beams with and without SBS. Figure 17 shows the results for Group A specimens. Also, Figure 18 represents the same curves for Group B specimens. The failure progression and ultimate failure stage for the two groups of beams are shown in Figure 19 to Figure 22 - Failure of Group B specimens for square panel and rectangular panel specimens, respectively.

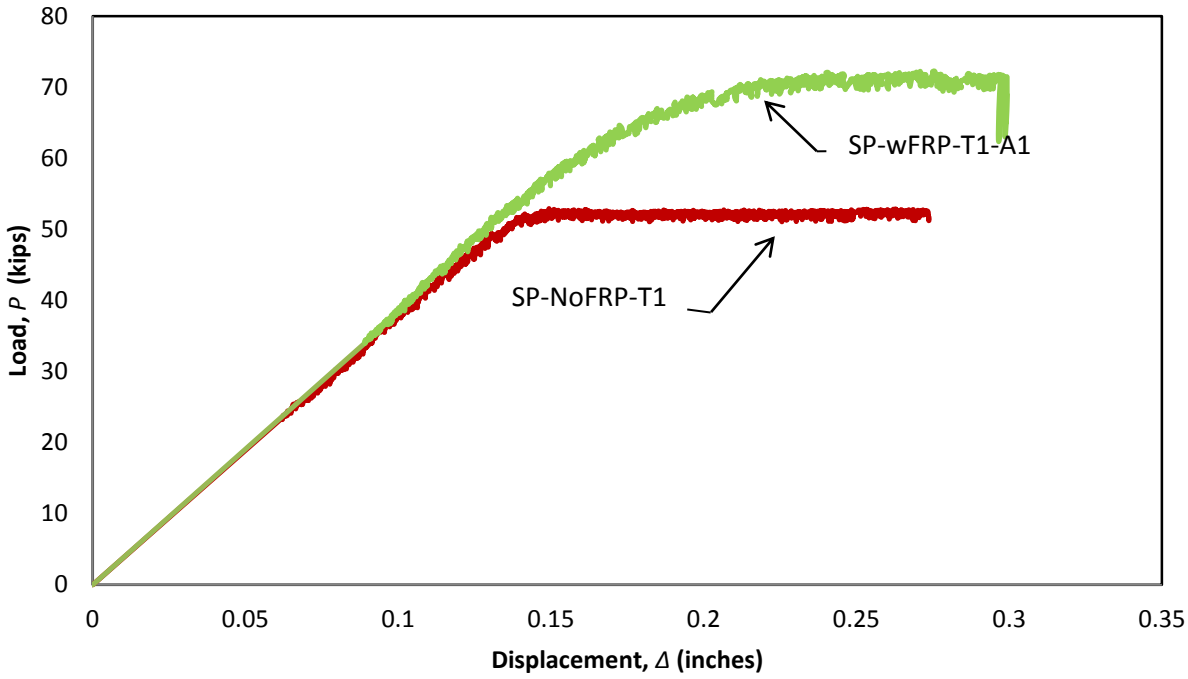

Figure 17 - Load-Displacement plot for tested square panel beams t_w=1/8”

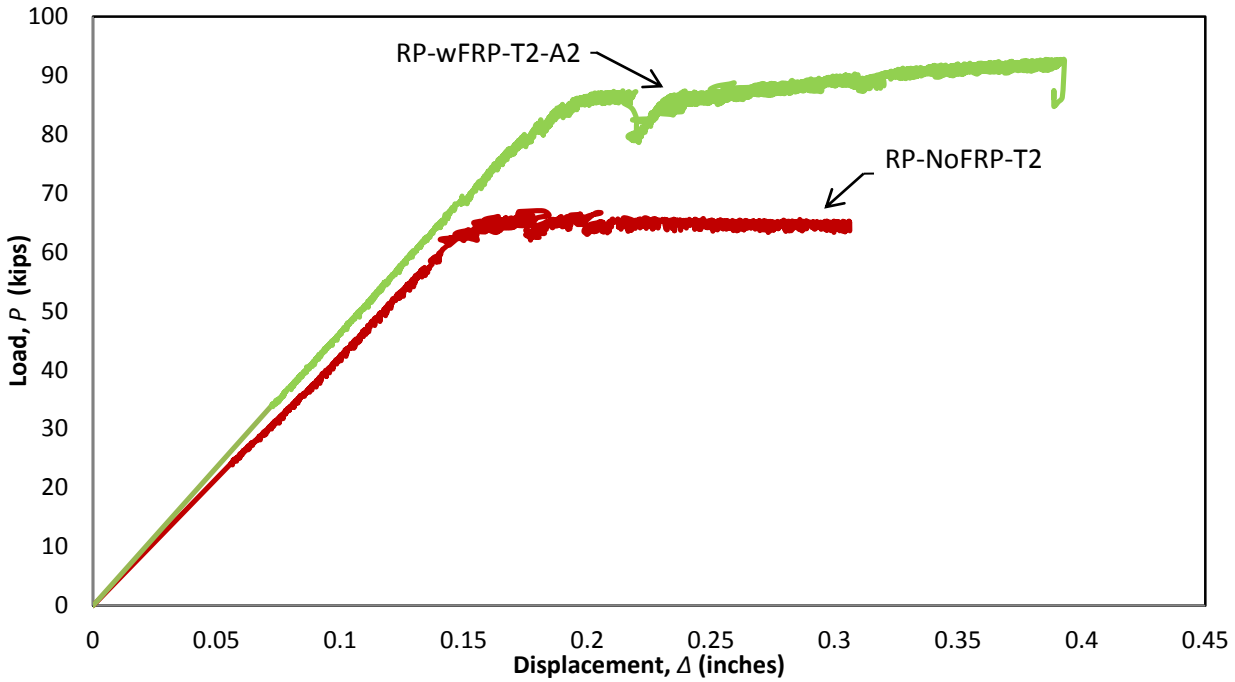

Figure 18- Load-Displacement plot for tested rectangular panel beams t_w=9/64”

3.5 Shear Capacity

Table 4 shows the maximum shear strength of tested beams in four different cases. Addition of GFRP stiffeners to the web of steel beams increases the shear capacity of section up to 36 and 38% for square panel and rectangular panel specimens respectively.

Table 4 – Shear capacity of tested beams

		Maximum Shear Strength	
Web Thickness (in)	Stiffening	Maximum Shear Strength	Percentage of Increase (%)
SP 1/8"	No Stiff.	39.67	-
	GFRP 3"Flange	54.18	36.57
RP 9/64"	No Stiff.	44.68	-
	GFRP 6"Flange	61.81	38.35

Load	Unstiffened Specimen	Stiffened Specimen
P= 0 kips		
P= 30 kips		
P= 50 kips		
P= 60 kips	Failed	

Figure 19– Failure progression for Group A specimens

(Table Continued)

Load	Unstiffened Specimen	Stiffened Specimen
P= 65 kips	Failed	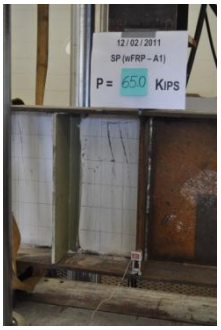
P= 70 kips	Failed	
P= 72.5 kips	Failed	

Load	Unstiffened Specimen	Stiffened Specimen
Front view at failure	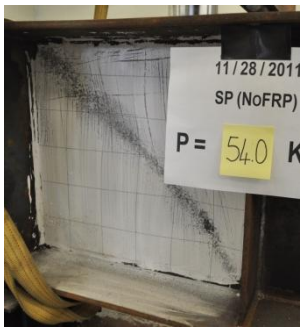	 
Back view at failure		
Crack in epoxy at failure		

Figure 20 – Failure of Group A specimens

Load	Unstiffened Specimen	Stiffened Specimen
P= 0 kips	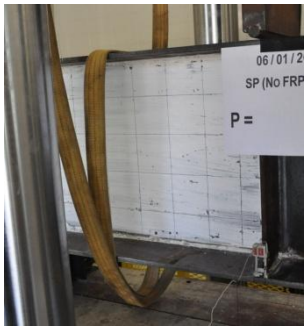	
P= 20 kips	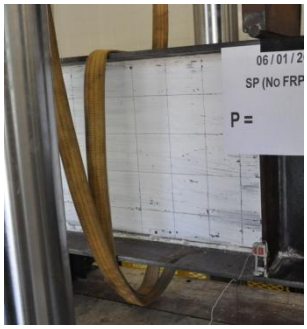	
P= 40 kips		
P= 50 kips		

Figure 21– Failure progression for Group B specimens

(Table Continued)

Load	Unstiffened Specimen	Stiffened Specimen
P= 60 kips		
P= 65 kips		
P= 70 kips	Failed	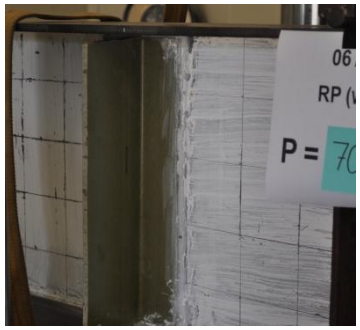
P= 75 kips	Failed	

(Table Continued)

Load	Unstiffened Specimen	Stiffened Specimen
P= 80 kips	Failed	
P= 85 kips	Failed	
P= 87.5 kips	Failed	
P= 89 kips	Failed	

(Table Continued)

Load	Unstiffened Specimen	Stiffened Specimen
P= 92.5 kips	Failed	

Load	Unstiffened Specimen	Stiffened Specimen
Front view at failure		
Back view at failure		

Figure 22 - Failure of Group B specimens

CHAPTER 4: FE MODELING

Experimental testing is the best method for investigating scientific problems. However, because of the costs and logistical issues associated with experimental testing, it is deemed unfeasible to rely solely on experimental testing. Therefore, a three dimensional (3D) finite element (FE) model that was developed at Louisiana State University (LSU) research group was used to expand the range of the parameters investigated in this study.

Two types of FE analysis were conducted in this study; namely "Eigenvalue Analysis", and "Nonlinear Analysis". Each of those types results in different kinds of useful information. The former one is often used in structural analysis to decompose complex behaviors in unique uncoupled ones. Eigenvalue analysis is basically done using transformations similar to those in dynamic analysis of structures where a unique eigenvalue corresponds to one of the structure's natural frequencies. In the unique buckling problems the mode shape from an eigenvalue analysis corresponds to the buckling mode of a structure. Every eigenvalue in the analysis corresponds to a unique load required to initiate the buckling for each mode. The buckling analysis using eigenvalue analysis is an elastic analysis and therefore, cannot be used to estimate failure strengths.

On the other hand, the nonlinear analysis is a monotonic static analysis, where materials and geometric nonlinearity is accounted for. The model designed based on this analysis type should demonstrate exactly the same behavior the experimental specimens show during the test in the lab. The initiation of buckling for perfectly symmetric structures and loads is not possible in this kind of analysis since the numerical models contrary to actual specimens have ideal geometries. In fact, imperfections such as distortions make the initiation of buckling possible. If buckling is not initiated, the specimen would theoretically fail by plasticization of the material

similar to a slender concentrically loaded column. In order to avoid this drawback, the results from eigenvalue analysis were used as imposed initial imperfections in the model by modifying the ideal geometry.

As mentioned earlier, a single point load was applied at the internal stiffener of each beam tested. It is important to mention, based on the loading pattern and the location the load was applied, the shear loading applied to the first panel is three times, and two times larger than applied to the other panels in group A and group B beams, respectively. Therefore, the reaction at the first constraint closer to the applied load is larger than the reaction to the further constraint in both groups of specimens.

The FE models were built and analyzed using the general purpose ANSYS package (Moaveni 1999). The models were validated using the experimental test results. After the model was validated, a parametric study was conducted.

A total of forty five cases were analyzed in ANSYS. Five web thicknesses of 1/8", 5/32", 3/16", 1/4", and 5/16" were chosen for square panel and rectangular panel cases. Each web thickness in the square panel group of specimens was modeled six times; (1) without stiffening, (2) with FRP stiffening (SBS) considering four different web flange widths, and (3) with steel stiffeners (SS). The two web thicknesses in rectangular panel beams were only modeled three times since just one GFRP web thickness was considered in that group compared to Group A with four different GFRP web Thicknesses. All of the dimensions of the models were exactly the same as the dimensions of experimented specimens expect the height of the models which were 20 inches.

Okeil et al., concluded that a vertical FRP stiffener is more suitable for SBS since it avoids unnecessary overloading of the stiffener if a compression-strut diagonal orientation (see

Figure 23) is used (Okeil et al. 2009b). Therefore, vertical orientation of GFRP stiffening was selected for experimental tests too.

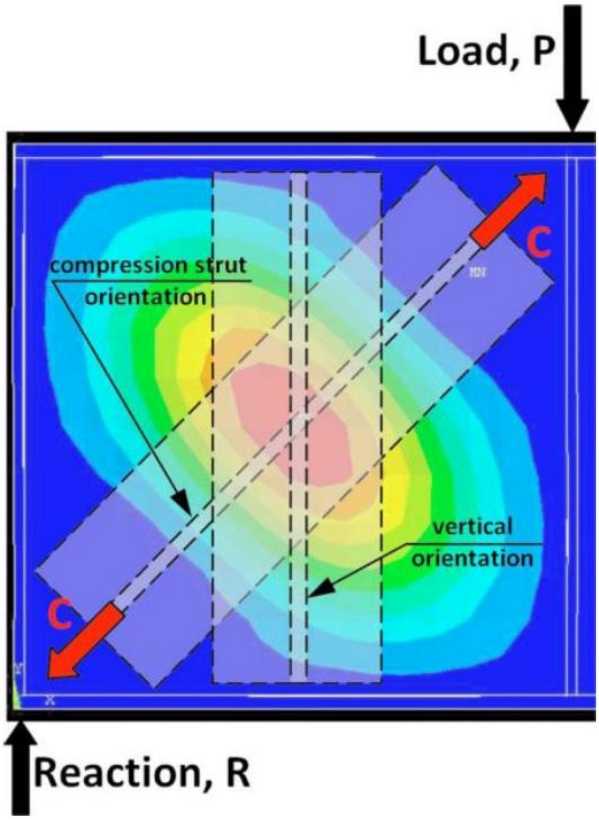

Figure 23 - Comparison of out of plane deformation contours for different orientations (Okeil et al. 2009b)

Figure 24 shows the FE meshes for the beam model without stiffening (Model I), with steel stiffening (Model II), and with GFRP stiffening (Model III).

The specimens corresponded to unstiffened models and GFRP stiffened models were tested in the lab experimentally; however, the steel stiffened beam cases were only analyzed and modeled in ANSYS. In Model II and Model III, the steel stiffener and the T-shaped GFRP stiffeners were added to both sides of the first panel of the steel beams, respectively.

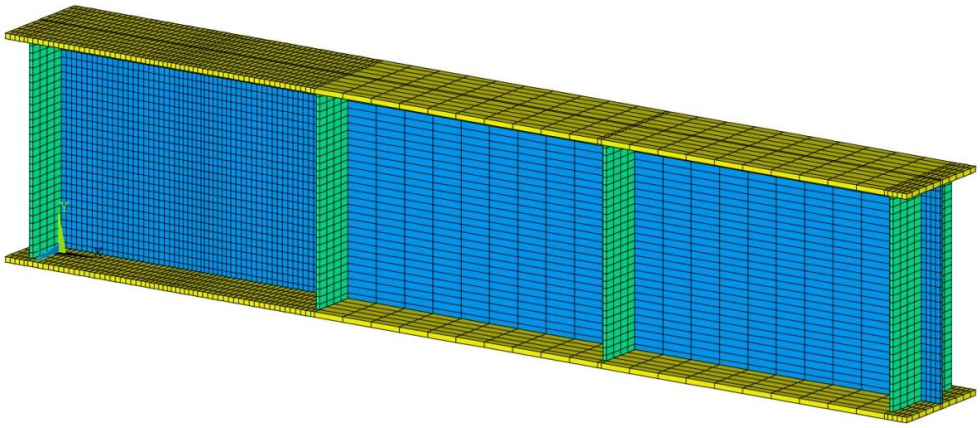

a – Unstiffened RP specimen

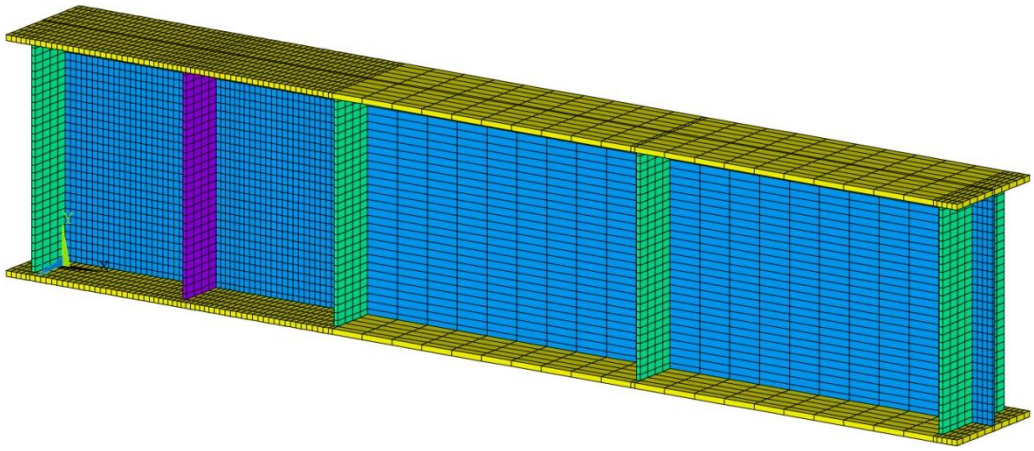

b – Steel stiffened RP specimen

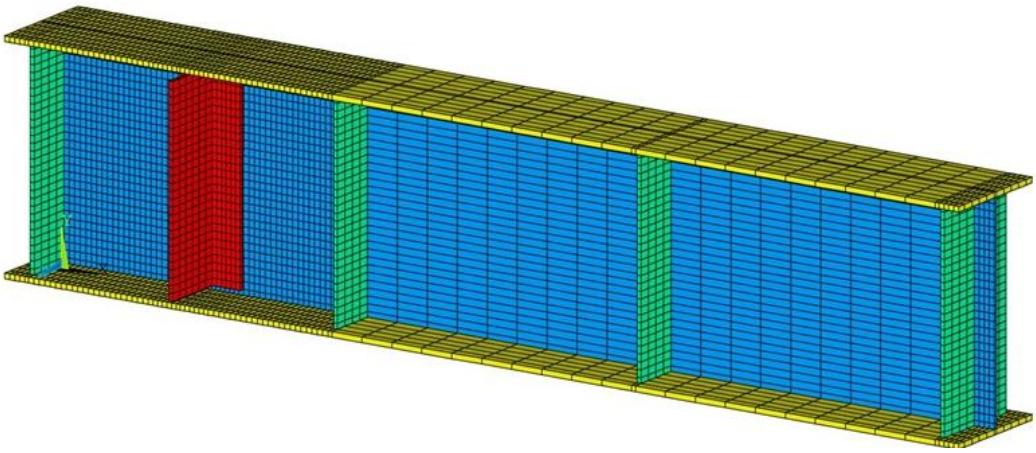

c – GFRP stiffened RP specimen

Figure 24 - Typical RP steel beam models used in the study

SOLID 65 elements were used to model steel, GFRP, and epoxy parts of the beams. Solid 65 is an eight-node solid element with three translation degrees of freedom at each node in the nodal x, y, and z directions. The element is capable of plastic deformation, cracking in three orthogonal directions, and crushing.

The experimentally applied load was distributing over two lines of nodes equal to the width of the flange above the first interior steel stiffener where the load tip lays on the top flange in the experimental tests. The boundary conditions and loads applied to the models are shown in Figure 25.

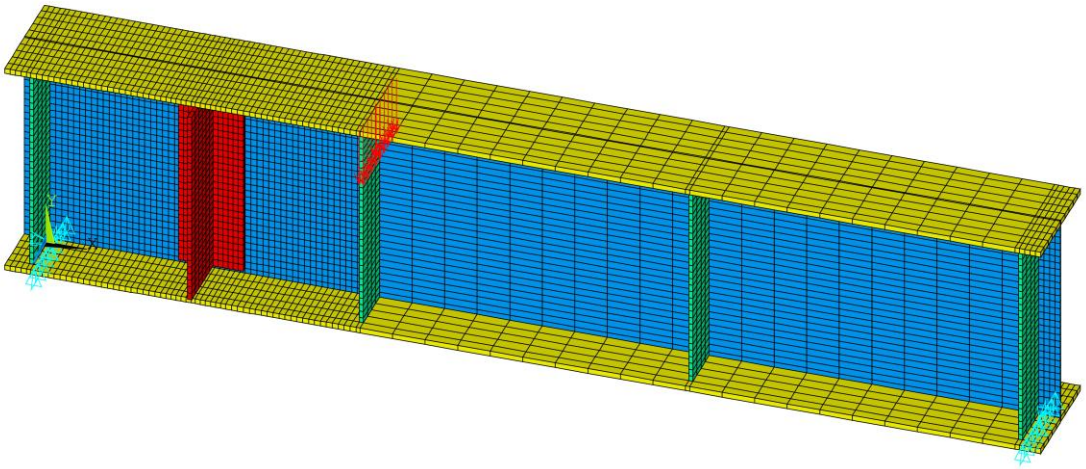

Figure 25 – Boundary conditions and load applied to the FE models

In order to make the model more dynamic, a flexible code was created to easily change the geometric properties of the beams and stiffeners without the need to remesh the entire beam-stiffener model (Broussard 2010). Geometric and material parameters were input is a script and the mesh was generated automatically.

4.1 Eigen Value Analysis

Using models discussed in previous section, an eigenvalue analysis was conducted where the first 3 mode shapes extracted as can be seen in Figure 26 for the unstiffened cases. The first mode was used in subsequent nonlinear analyses as an imposed distortion to the beam.

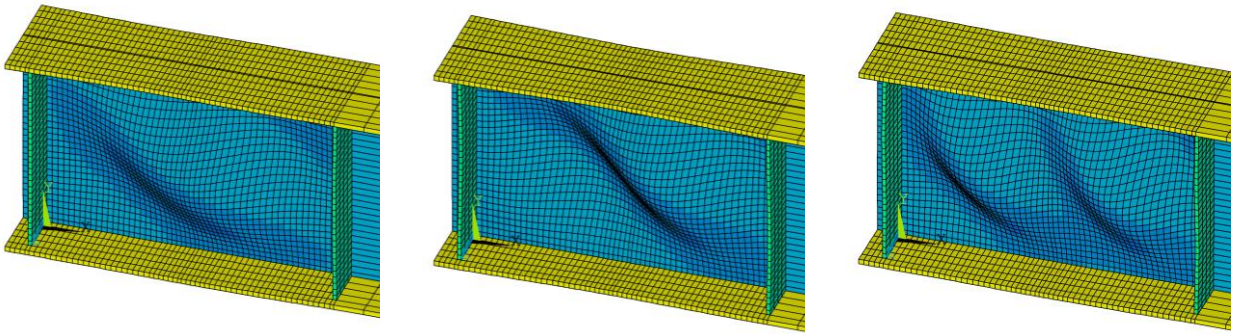

a- First mode b- Second mode c- Third mode

Figure 26 - First mode shapes for unstiffened cases

Similar runs were conducted for the models with steel stiffeners and with FRP stiffeners. The first mode for these cases can be seen in Figure 27.

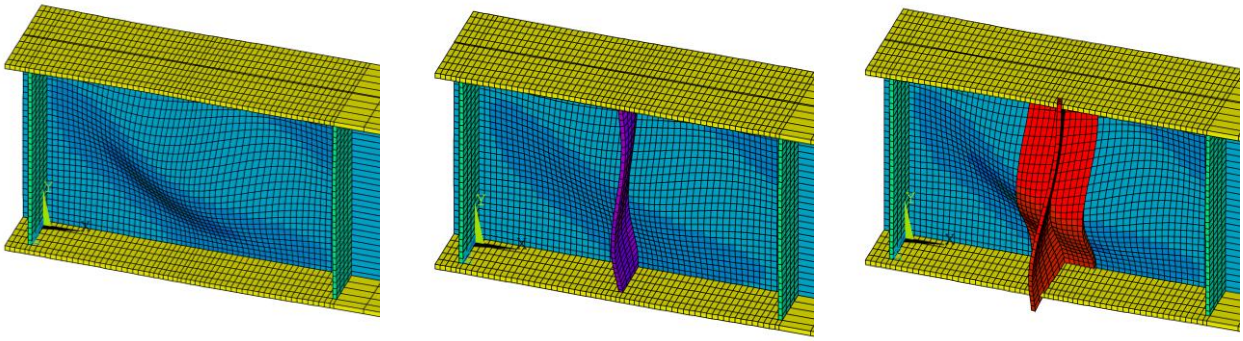

a- Unstiffened case b- Steel Stiffened case c- SBS case

Figure 27 - First mode shapes for different cases

4.2 Modeling of Debonding

By ignoring debonding in the FE models the analysis will not be capable of simulating the experimentally observed mode of failure, which may lead to overestimating the shear strength. Therefore, one of the most important and critical aspect of the analysis is the modeling of the epoxy bonding the GRFP stiffener to the steel beam's web. In the literature and in earlier experimental investigations, it was revealed that the debonding of the GFRP stiffener was the dominant failure mechanism. Therefore, precise representation of this behavior in the finite element modeling is of great importance to the accuracy of the results. An ultimate rupture strain for epoxy was set in ANSYS in order to simulate the actual failure mechanism. Epoxy elements exceeding the ultimate rupture strain were removed at the end of each of the displacement steps using an ANSYS 'KILL' command. The debonding initiates from the corners of the contact area and propagates to the sides of the stiffener flange. Ultimately, the only attached part of the epoxy to the web is the central part of the contact area which is eventually detached suddenly due to the high strains. Figure 28 depicts a typical progression of the epoxy element elimination in the FE model.

4.3 Model Validation

Four experimentally tested specimens were modeled using the developed FE model. The load-deflection plots of Groups A and B are shown in Figure 29 and Figure 30 which are pretty similar to the P-Δ plots of experimental specimens. Table 7 shows a summary of the experimental shear capacities resulted by SBS technique and the shear capacity values derived based on the FE modeling of the tested specimens using actual values of dimensions. The average ratio of estimated shear capacity to the shear capacity resulted by experimental tests, V_{val}/V_{exp}, is almost equal to 0.99 with a very small standard deviation for rectangular panel

specimens. Also, similar ratios can be observed for square panel beams with tolerance of ±6% from being one, meaning the validated values are strongly close to the values achieved by the experimental tests. Therefore the FE modeling was highly successful in imitating the model and can be used to estimate the behavior of the similar models perfectly.

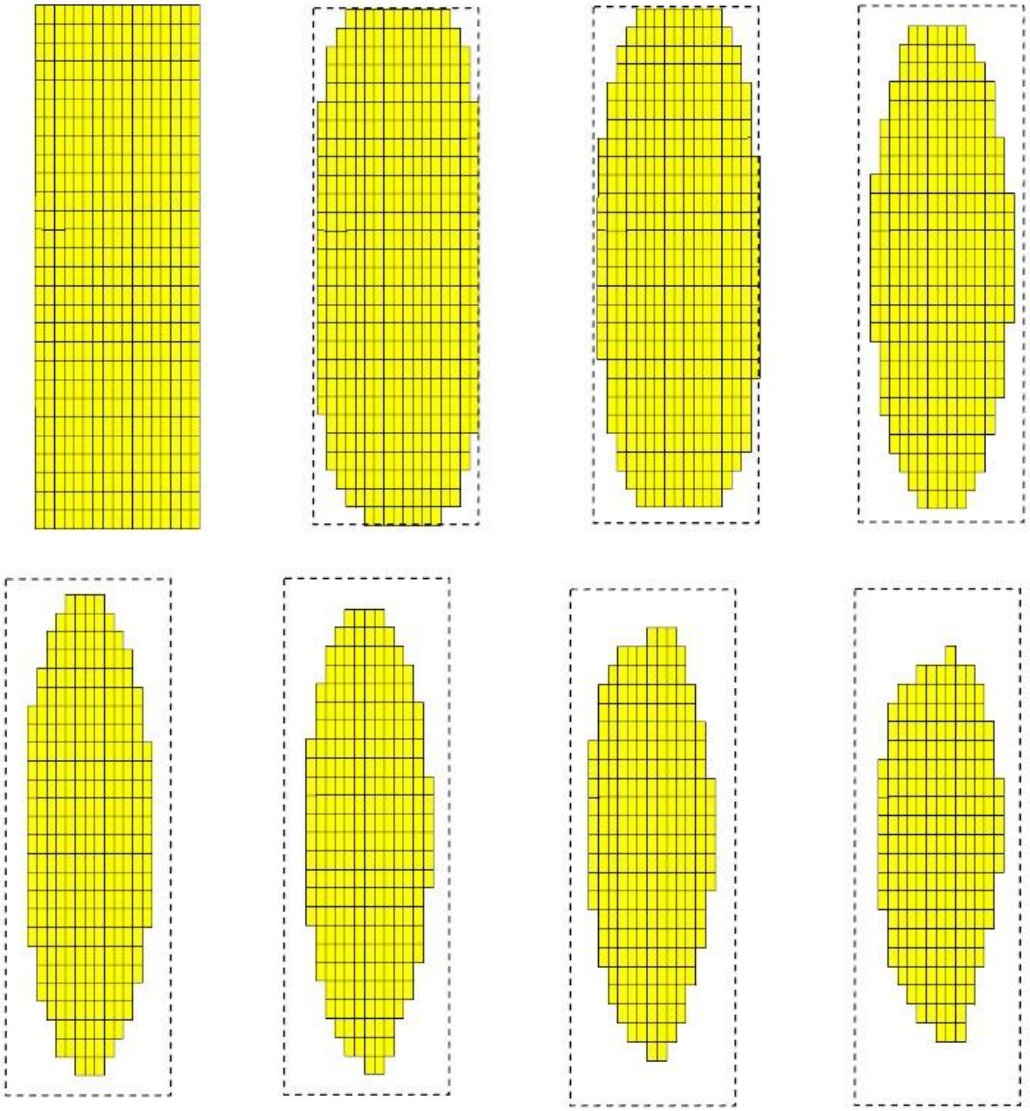

Figure 28 - Modeling of deboning in ANSYS (Broussard 2010)

Moreover, the deformed shapes of the beams after failure for the four different cases are depicted in Figure 31 and Figure 32, respectively. It can be seen, the observed progression of

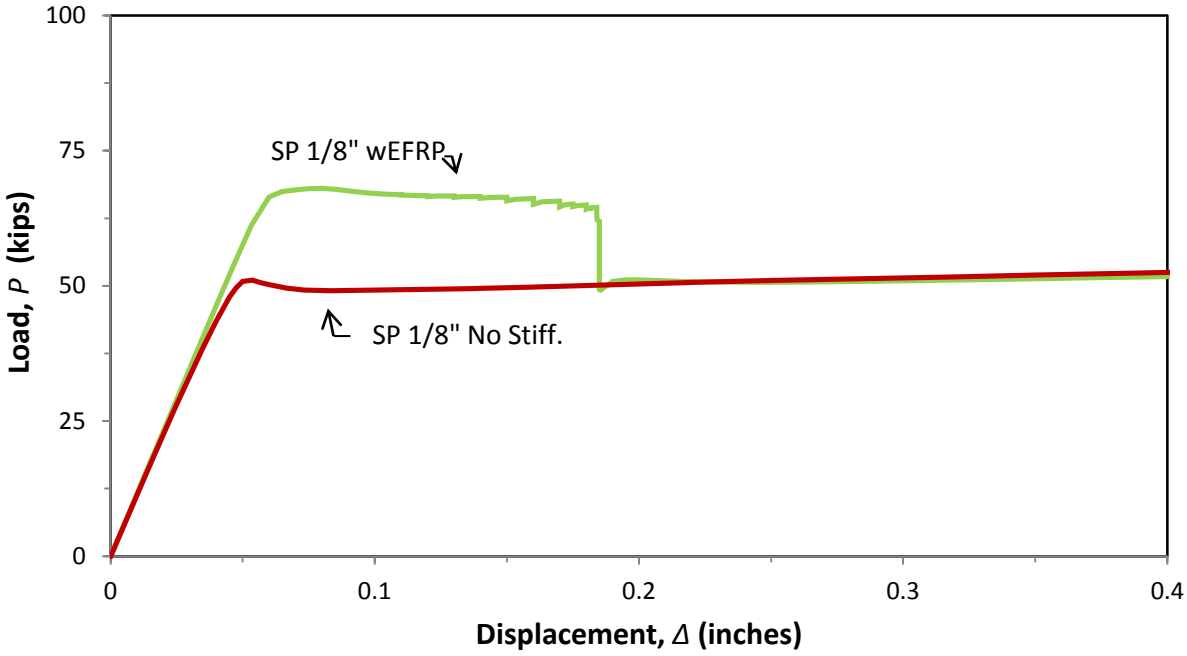

Figure 29 – Model-predicted Load-Displacement plot for SP specimens t_w=1/8”

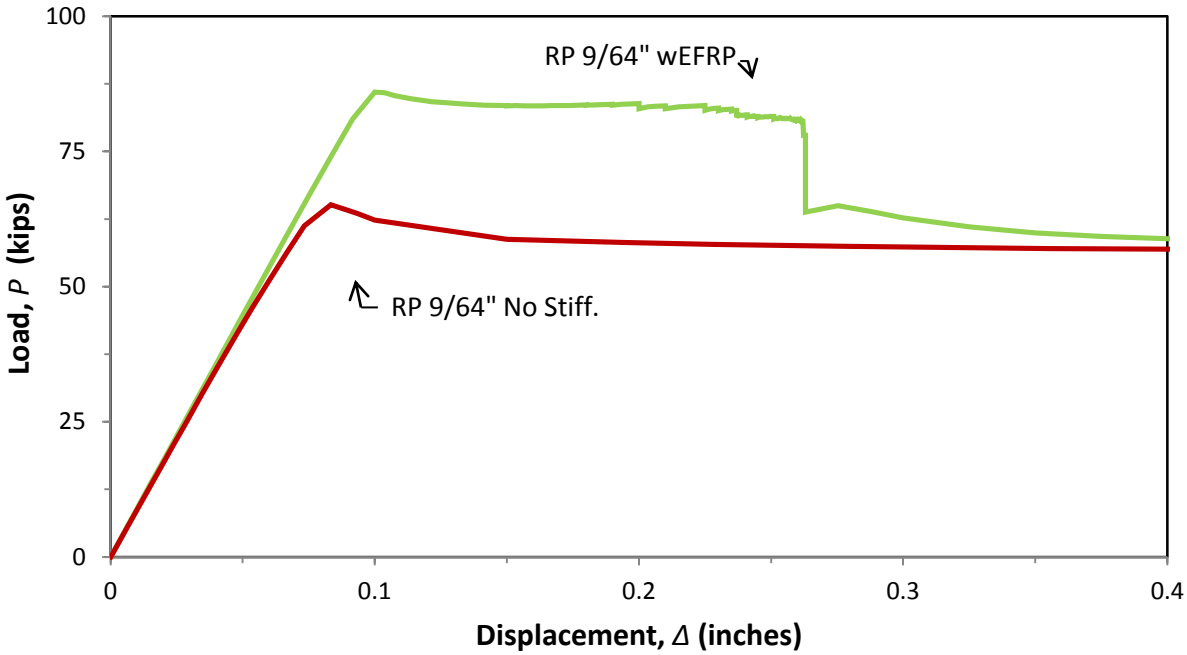

Figure 30 - Model-predicted Load-Displacement plot for RP specimens t_w=9/64"

buckling and deformed shapes of the specimens after failure for all four tested beams and their relative FE model deformed shapes are identical.

Table 5 - Comparison of experimental and validation results

Maximum Shear Strength				
Web Thickness (in)	Stiffening	Maximum Shear Strength		V_{val}/ V_{exp}
		Experiment	Validation	
SP 1/8"	No Stiff.	39.67	41.17	1.04
	GFRP 3" Flange	54.18	51.01	0.94
RP 9/64"	No Stiff.	44.68	43.42	0.97
	GFRP 6" Flange	61.81	61.67	1.00

4.4 FE Results

Analysis results are presented in the form of load-displacement, P-Δ plots. The parametric study covered (1) unstiffened, (2) reinforced with vertical GRFP stiffeners, and (3) stiffened with steel stiffener on each side of the critical web panel. In an earlier study by Broussard (2010), four different flange widths were considered for square panel cases to investigate the effect of changing the contact area of GFRP stiffener for different web slendernesses.

The GFRP stiffener flange widths considered for each beam web thickness in square panel cases were 3 inches, 4 inches, 6 inches, and 8 inches. In the current study, only one flange width (6”) is considered as it was revealed that flange widths in the predicted range (6” as delivered) have little impact on behavior. Moreover, an additional case for steel stiffener, web thickness of 0.375 inch, was analyzed as part of the parametric study. Figure 33 to Figure 37 show the relationship between load and deflection of stiffened and unstiffened specimens of Group A, square panel specimens. On the other hand, Figure 38 to Figure 42 show the P-Δ relationship between stiffened and unstiffened specimens of Group B, rectangular panel beams. These plots represent the responses of unstiffened or stiffened beam under the action of a point load applied monotonically along the top flange of the simply supported beam at a quarter point along the

span length. The deflection values are measured at the same point of load application along the top flange of the beam.

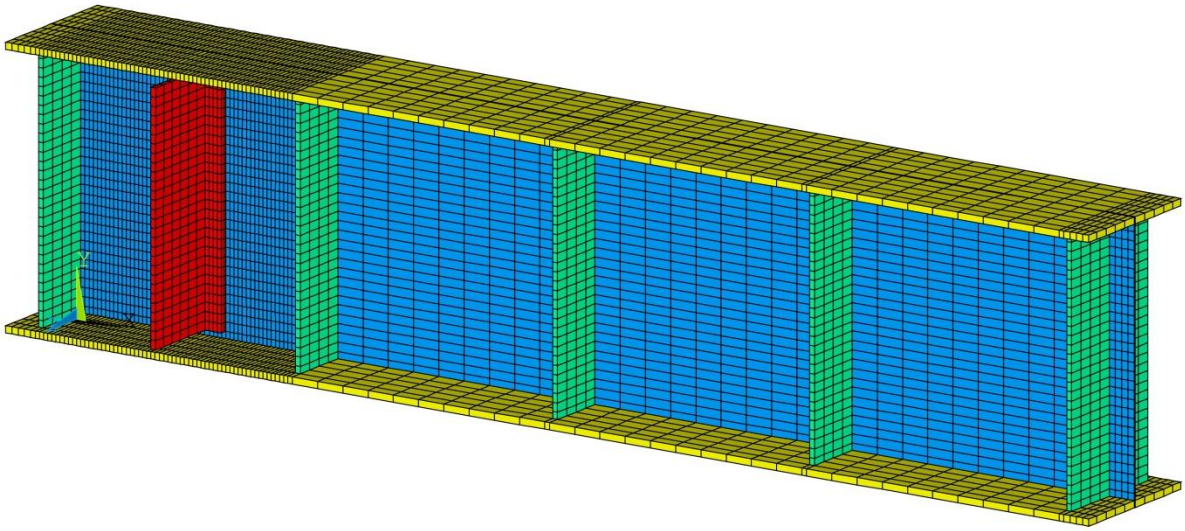

a- Finite Element mesh used in analyses of experimented SP specimens

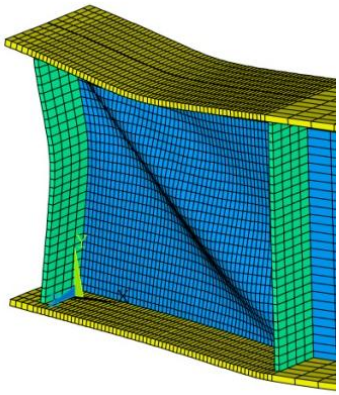

b- Specimen with no stiffener at failure

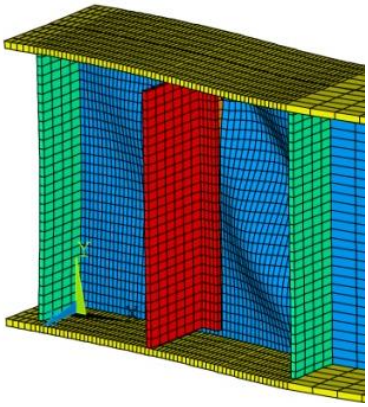

c- Specimen with FRP stiffener at debonding

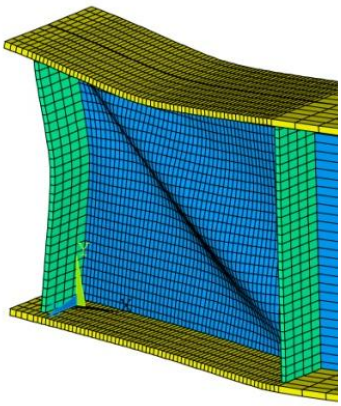

d- Specimen with FRP stiffener at failure

Figure 31- Deformed shapes of the experimented square panel beams

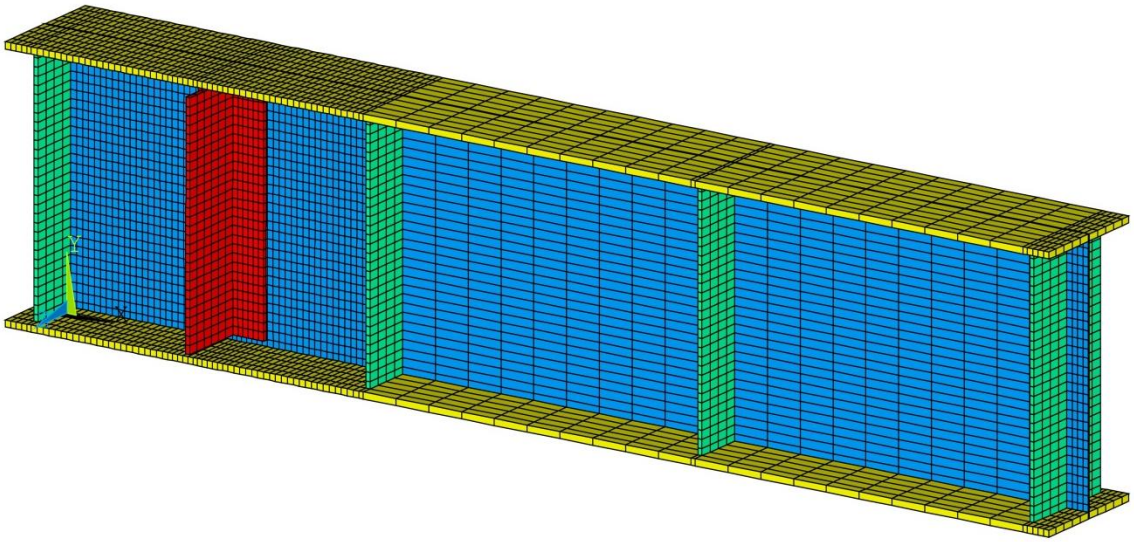

a- Finite Element mesh used in analyses of experimented RP specimens

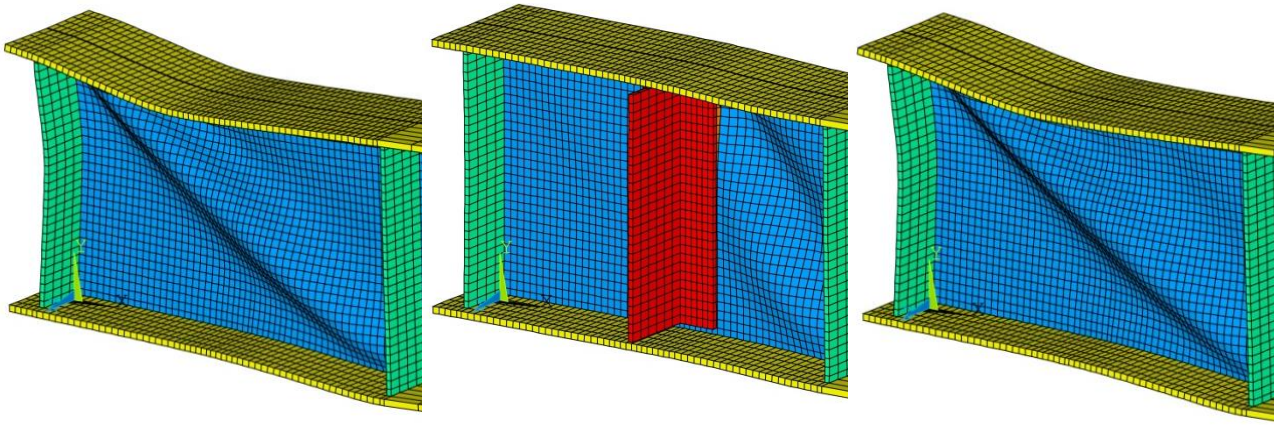

b- Specimen with no stiffener at failure

c- Specimen with FRP stiffener at debonding

d- Specimen with FRP stiffener at failure

Figure 32- Deformed shapes of the experimentally tested rectangular panel beams

Figure 43 shows the FE mesh used in eigenvalue and nonlinear analyses of rectangular panel cases with web thickness of 5/16". It also displays the deformed shapes after failure of

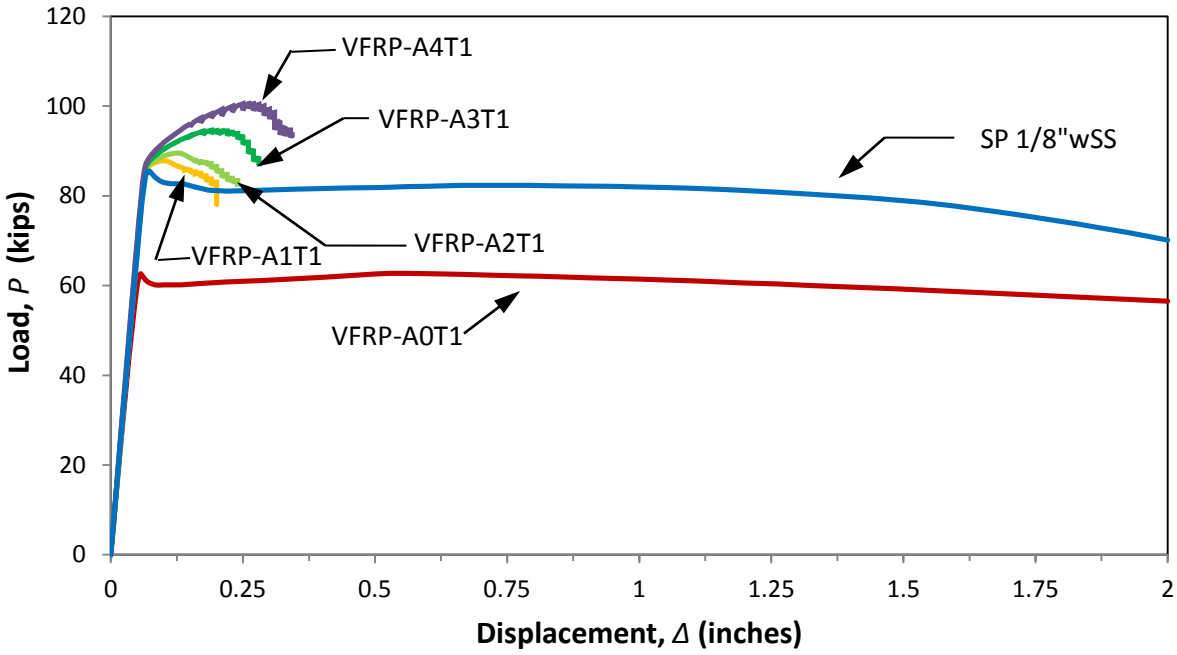

Figure 33- Load-Displacement plot for square panel beam t_w=1/8”

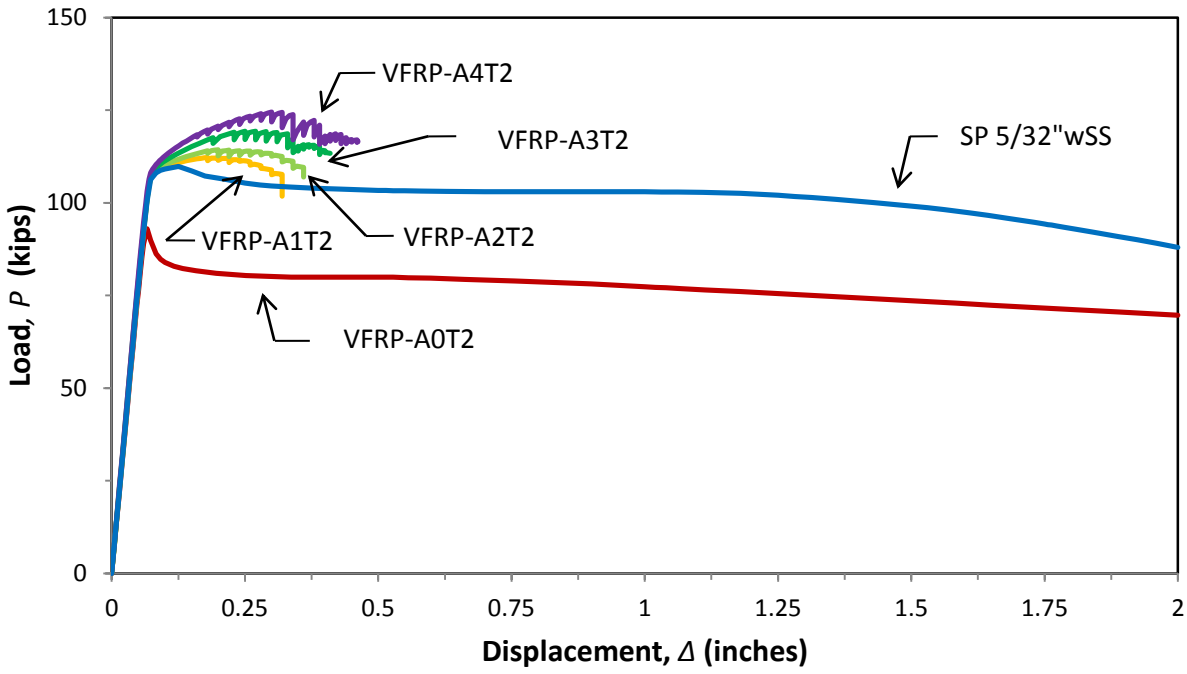

Figure 34 - Load-Displacement plot for square panel beam tw=5/32”

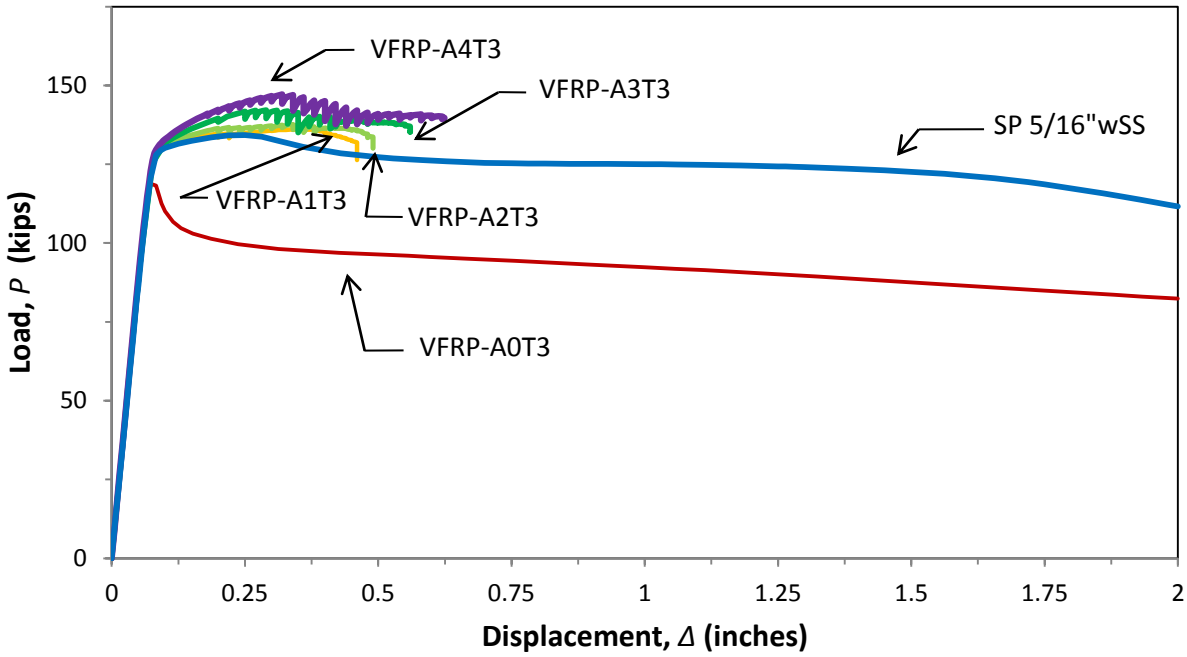

Figure 35 - Load-Displacement plot for square panel beam t_w= 3/16”

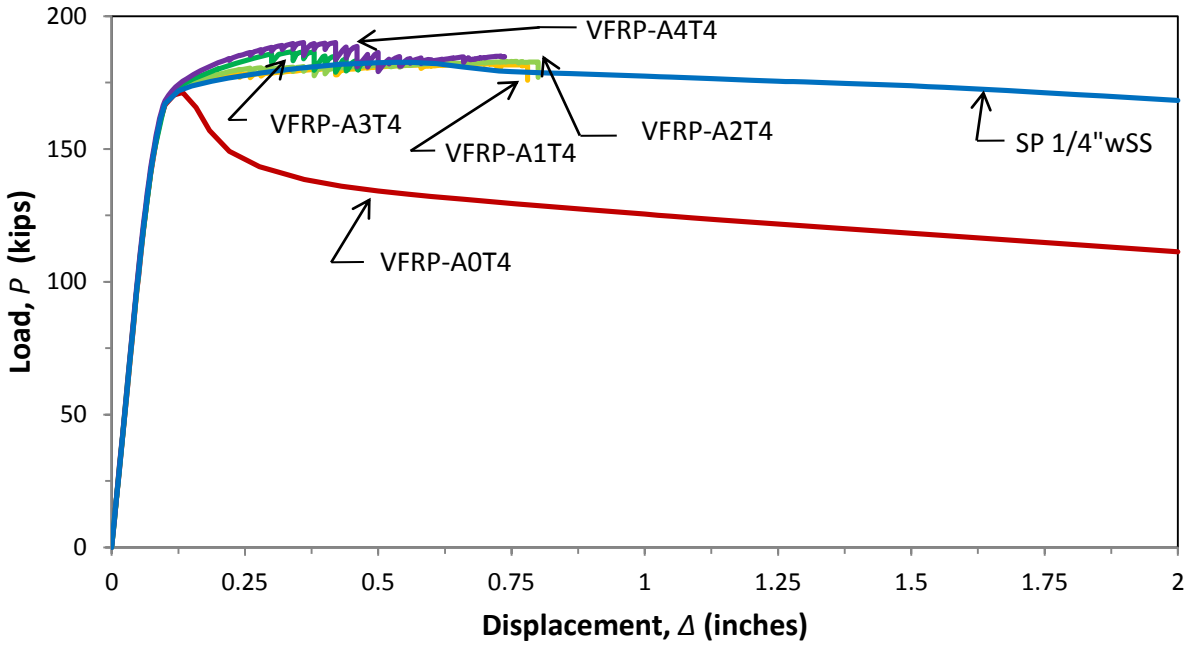

Figure 36- Load-Displacement plot for square panel beam t_w=1/4”

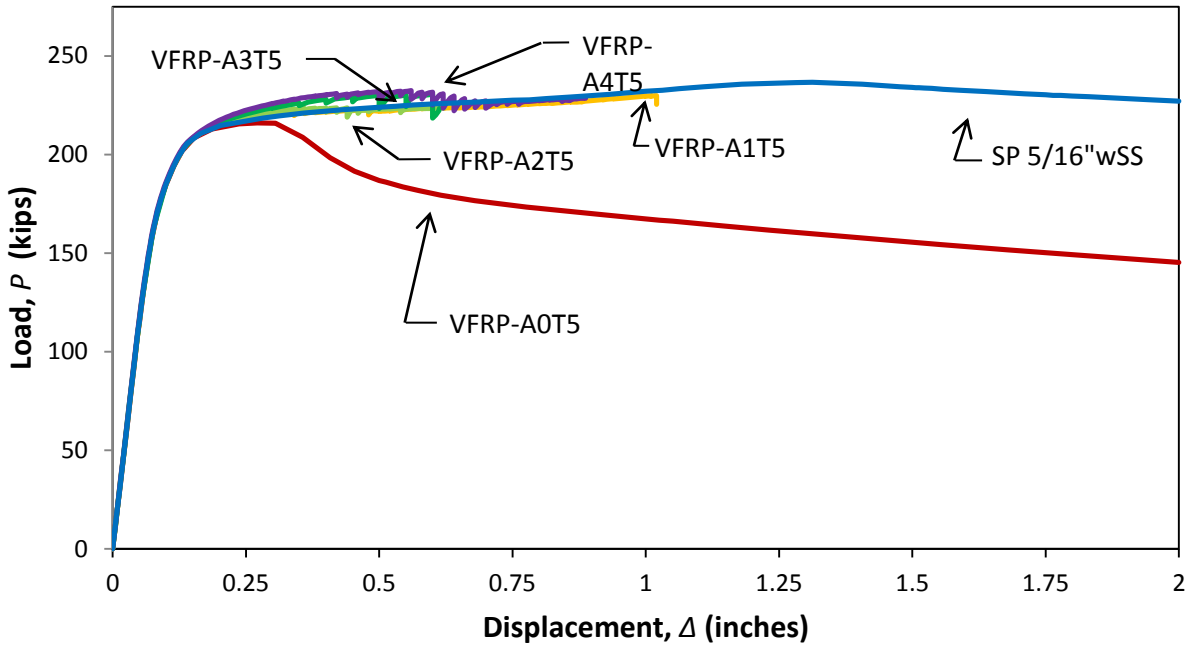

Figure 37 - Load-Displacement plot for square panel beam t_w=5/16”

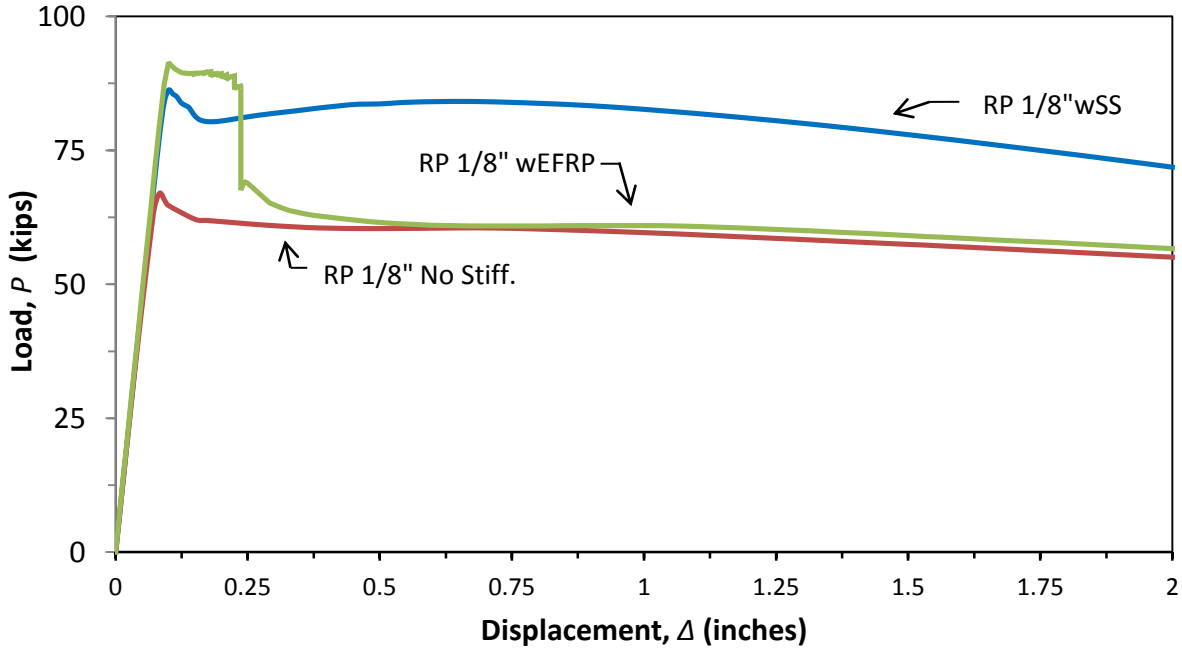

Figure 38- Load-Displacement plot for rectangular panel beam t_w=1/8”

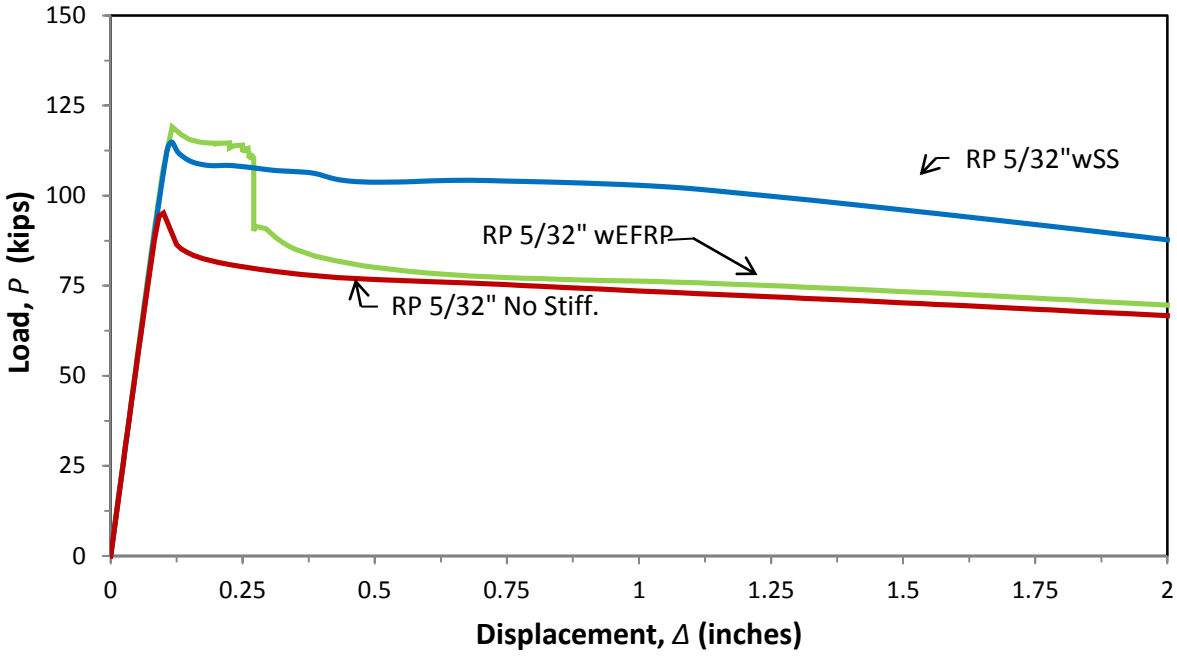

Figure 39- Load-Displacement plot for rectangular panel beam t_w=5/32”

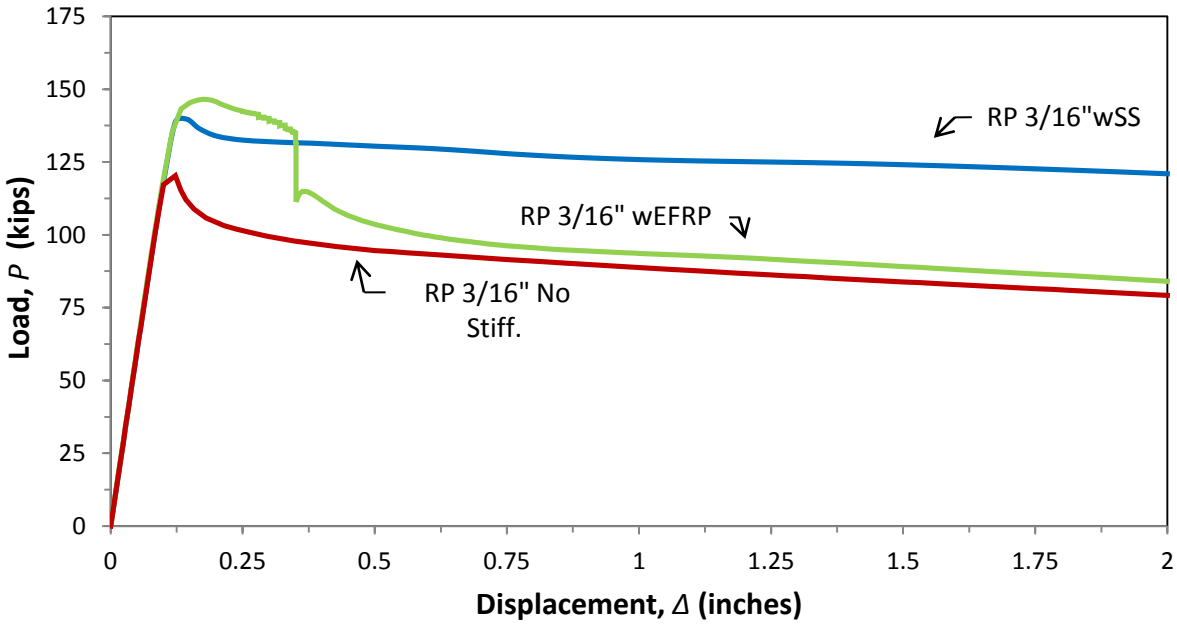

Figure 40 - Load-Displacement plot for rectangular panel beam t_w=3/16”

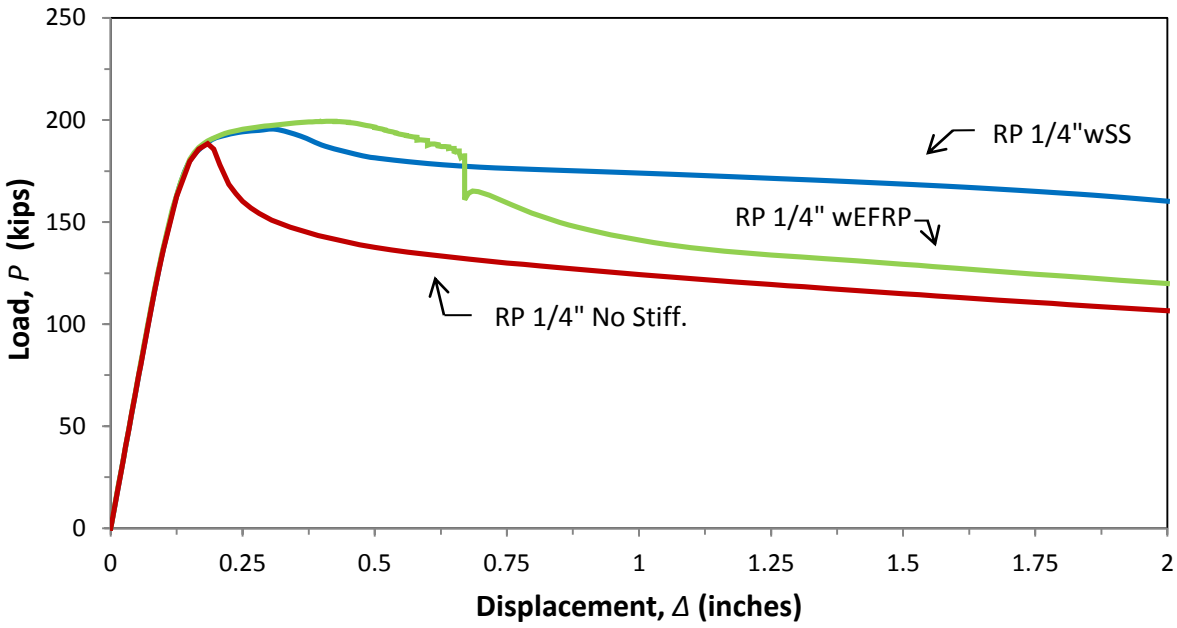

Figure 41 - Load-Displacement plot for rectangular panel beam t_w=1/4”

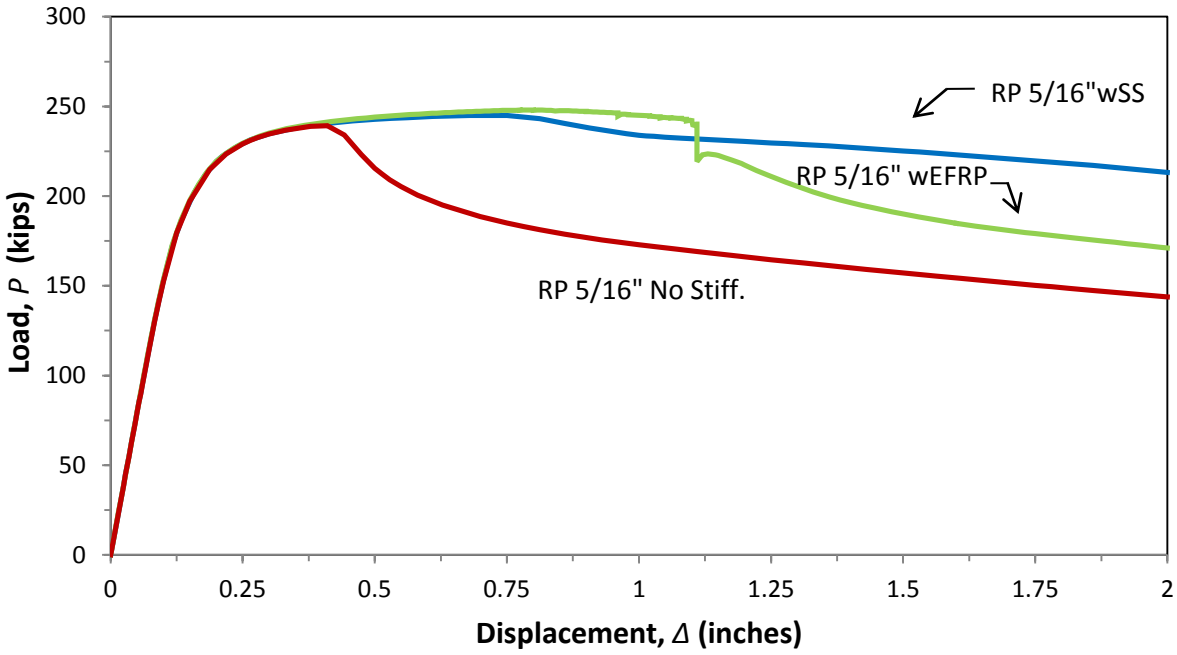

Figure 42- Load-Displacement plot for rectangular panel beam t_w=5/16”

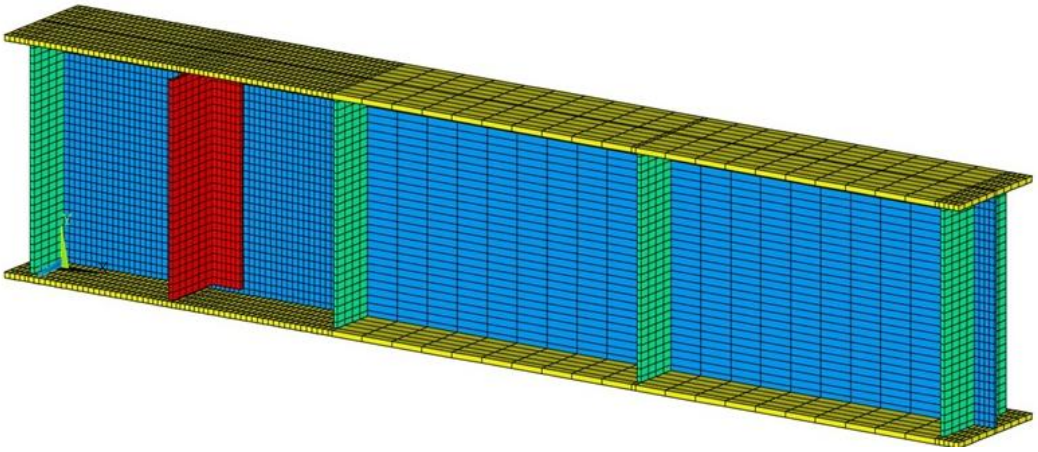

Finite Element mesh used in eigenvalue and nonlinear analyses of RP specimens

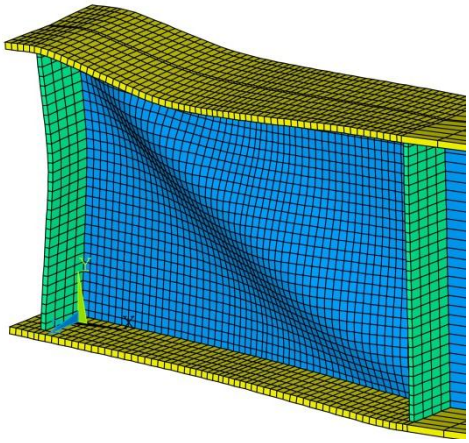

b- Specimen with no stiffener

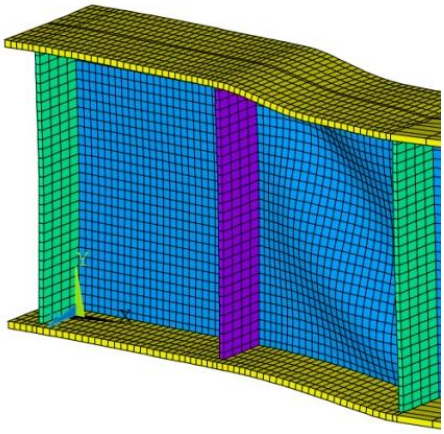

c- Specimen with steel stiffener

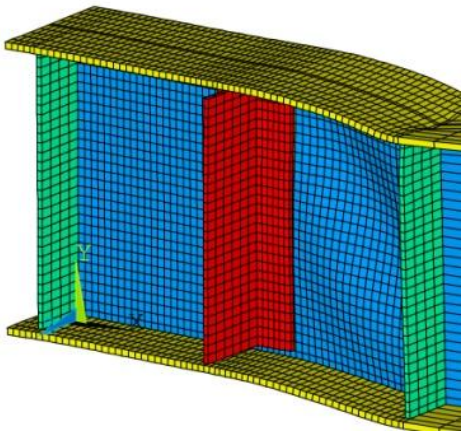

d- Specimen with FRP stiffener at debonding

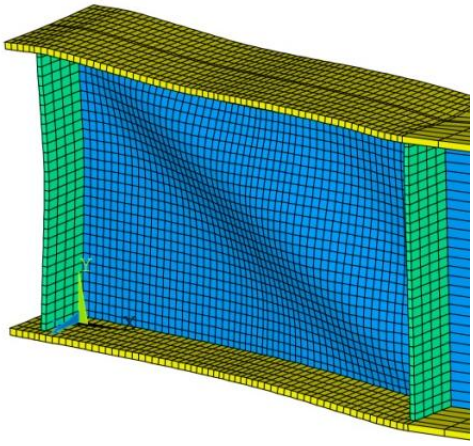

e- Specimen with FRP stiffener at failure

Figure 43 - Deformed shapes of RP specimens t_w=5/16”

each specimen in three different cases of stiffening; (1) no stiffening, (2) steel stiffening, and (3) FRP stiffening (a) at debonding, and (b) FRP stiffening at failure. The reason for selecting aforementioned web thicknesses is the closeness of these thicknesses to the actual web thicknesses of the tested beams.

4.5 Shear Capacity

Table 6 and Table 7 summarize the results of the analyses performed in the parametric study. The ranges of increases in analytical ultimate load attained for each beam are shown. As expected, the greatest increases in ultimate load in both groups of specimens are found in the beams with the most slender webs. The GFRP stiffeners are most effective in stabilizing the webs that are more susceptible to out of plane buckling. The highest ultimate load increase is 66% for the 1/8" web beam stiffened with an 8" flange GFRP stiffener, which shows that significant increases can be attained in beams with slender webs. Increases in shear capacity for beams governed by shear yielding are also possible; however at a significant lower level.

An interesting observation can be drawn from these results that in almost all cases, except the 5/16" web thickness in square panel specimens, the ultimate load increase due to GFRP stiffening is higher than the increase caused by steel stiffening. This indicates that contrary to expectations the efficiency of SBS is at least at the same level as steel stiffening.

Table 6 - Summary of Shear Capacity Analysis Results for Square Panel Specimens

Ultimate Load (kips)								
Web Thickness (in.)	$V_{NoStiff.}$	V_{FRP}				V_{SS}	Ultimate Load Increase Range Due to GFRP Stiffening (%)	Ultimate Load Increase Due to Steel Stiffening (%)
	Unstiffened Beams	GFRP Stiffened Beams				Steel Stiffened Beams		
		3" Flange	4" Flange	6" Flange	8" Flange			
1/8"	44	64	65	70	73	65	44-66	47
5/32"	64	84	85	89	93	81	32-46	27
3/16"	89	102	103	106	110	99	15-24	12
1/4"	128	136	137	139	142	134	6-11	5
5/16"	162	172	167	172	174	188	6-8	16

Table 7 - Summary of Shear Capacity Analysis Results for Rectangular Panel Specimens

Ultimate Load (kips)					
Web Thickness (in.)	$V_{NoStiff.}$	V_{FRP}	V_{SS}	Ultimate Load Increase Due to GFRP Stiffening (%)	Ultimate Load Increase Due to Steel Stiffening (%)
	Unstiffened Beams	GFRP Stiffened Beams 6" Flange	Steel Stiffened Beams		
1/8"	44	60	57	36	28
5/32"	63	79	76	25	21
3/16"	80	97	93	22	16
1/4"	125	132	130	6	4
5/16"	159	164	163	3	2

CHAPTER 5: RESULTS AND DISCUSSION

In this chapter more details about the results from the experimental program and the parametric study are presented and further discussed.

5.1 Experimental Study Results

5.1.1 Behavior Description

It can be seen from the load-deflection plots (Figure 17 and Figure 18) that the use of GFRP sections not only improves shear strength of the steel beams, but also enhances the stiffness of SBS specimens. The increase in the stiffness is the result of introducing the GFRP stiffeners whose axial and more importantly flexural rigidity is inherently higher than the unstiffened steel web. Therefore, when the stiffened specimen is subjected to high shear loads and consequently out-of-plane buckling, the GFRP starts to act against the buckling and maintain the elastic behavior of the section. Conversely the unstiffened specimens are not able to maintain the elastic behavior and start to yield under such high loads.

SBS strengthening delays the onset of yielding which provides a larger elastic energy for the stiffened specimen compared to the unstiffened one. After yielding, a clear plateau is evident for both strengthened and unstrengthened specimens; however, the deformation ductility and energy ductility is less for GFRP stiffened beams compared to the unstiffened ones.

5.1.2 Predicting Shear Capacity Using Code Equations

The LRFD Manual for Steel Construction (AISC 2001) and the LRFD Bridge Design Specifications (AASHTO 2004) suggest almost identical shear provisions in order to calculate the nominal shear capacity of the tested beam theoretically. In this study, the bridge design code (AASHTO 2004) was selected to predict the shear capacity of tested beams and FE models. The bridge design code is more appropriate for the studied cases since most of the built-up sections

are common in this industry rather than in the building construction. According to AASHTO (AASHTO 2004), the plastic shear strength, V_p, of a built-up section is equal to

$$V_p = 0.58\, F_{yw}\, D t_w \tag{1}$$

where F_{yw}=yield strength of the web; D=web depth; and t_w =thickness. The nominal shear resistance of the web is given as

$$V_n = C\, V_p \tag{2}$$

in which C is a coefficient that depends on the properties of the web and d_o=distance between transverse stiffeners. The plastic strength can only be fully achieved (i.e., C=1.0) if the buckling induced modes of failure are prevented from taking place. There are three possible stages for the failure defined by the code in which C is reduced as the web slenderness increases. These stages are

$$C = 1.0 \text{ for } \frac{D}{t_w} \leq 1.12\sqrt{\frac{Ek}{F_{yw}}} \tag{3.a}$$

$$C = \frac{1.12}{D/t_w}\sqrt{\frac{Ek}{F_{yw}}} \text{ for } 1.12\sqrt{\frac{Ek}{F_{yw}}} < \frac{D}{t_w} \leq 1.40\sqrt{\frac{Ek}{F_{yw}}} \tag{3.b}$$

$$C = \frac{1.57}{(D/t_w)^2}\frac{Ek}{F_{yw}} \text{ for } \frac{D}{t_w} > 1.40\sqrt{\frac{Ek}{F_{yw}}} \tag{3.c}$$

where, E=web's modulus of elasticity and k is given as

$$K = 5 + \frac{5}{({}^{d_0}/_{D})^2} \tag{4}$$

A value of 1.0 should be considered for the slenderness which satisfies Eq. (3.a), where shear yielding is the failure mode. Otherwise, the values of C can be calculated using Eqs. (3.b) and (3.c) where inelastic and elastic buckling modes are the failure modes respectively.

According to Equations (1) to (4) and Table 8, the buckling mode of all specimens except the stiffened square panel is elastic. Stiffening of the bare steel web with GFRP increases the *C* value from 0.41 to 0.89, and shifts the buckling mode from elastic to inelastic. Therefore, the nominal value of the shear strength increases from 20.43 to 43.96 kips.

Table 8 – Nominal shear resistance of the tested specimens according to AASHTO

Nominal Shear Resistance of the Tested Specimens								
Web Thickness (in)	Stiffening	$\frac{D}{t_w}$	$1.12\sqrt{\frac{Ek}{F_{yw}}}$	$1.40\sqrt{\frac{Ek}{F_{yw}}}$	C	V_p (kip)	V_n (kip)	Failure Mode
SP 1/8"	No Stiff.	164.62	94.44	118.05	0.41	49.61	20.43	Elastic
	GFRP 3" Flange	164.62	145.89	182.36	0.89	49.61	43.96	Inelastic
RP 9/64"	No Stiff.	147.22	80.15	100.18	0.37	58.67	21.76	Elastic
	GFRP 6" Flange	147.22	108.68	135.85	0.68	58.67	40.02	Elastic

Estrada et al. stated that ignoring the contributions of flanges and stiffeners after buckling results in underestimating the shear capacity of steel beams which may clarify the inconsistency between the codes predicted and measured shear strengths for unstiffened beams (see Table 8) (Estrada et al. 2007).

At this moment, no code provisions exist for calculating shear capacity of GFRP stiffened beams. However, AASHTO shear capacity equations can be used for estimating the shear capacity of SBS strengthened beams by assuming that the GFRP stiffeners behave similar to steel stiffeners welded at the same location, i.e., middle of critical web panel, which divides the panel into two equal panels having the width equal to half of the original panel's width. The applicability of current code equations for estimating the capacity of SBS-Strengthened beams is justified by the fact that an efficiency coefficient of 1.04 and 1.03 was established for SP and RP beams, respectively. In summary, the predicted failure mode for the square panel specimen is altered from being initiated by elastic buckling for the unstiffened specimens to inelastic

buckling or shear yielding for the SBS strengthened specimens. For the rectangular panel beam, the buckling mode is not altered; however, the value of *C* and consequently the nominal shear strength is increased. Therefore, based on the existing code provisions for steel, the SBS technique can enormously increase the nominal shear strength of steel beams by utilizing the plastic shear capacity of the beams especially for slender web thicknesses.

5.1.3 Deformation Ductility

Studying the P−Δ relationship from a ductility point of view shows that the increase in strength is accompanied by a reduction in ductility. In general, this reduction is typical of FRP strengthening. Despite the reduced ductility, SBS strengthened beams are not perfectly brittle and are capable of absorbing a significant amount of inelastic energy. Table 9 lists the deformation ductility estimates for the tested specimens. Deformation ductility is defined as the ratio of the deformation at failure to the deformation at the proportional limit.

It should be noted that the tests were stopped manually at certain deformations (0.5 in.) after yielding to avoid excessive failure of the specimens. Yet, SBS-strengthened specimens' ductility exhibited less deformation compared to unstiffened ones. It can also be seen that a slight improvement in the deformation ductility is exhibited by specimens with thicker web and/or longer bond area.

Table 9 – Deformation ductility for the tested specimens

Deformation Ductility		
Web Thickness (in)	Stiffening	Tested Specimens Deformation Ductility
SP 1/8"	No Stiff.	1.97
	GFRP 3" Flange	1.58
RP 9/64"	No Stiff.	2.13
	GFRP 6" Flange	2.07

5.1.4 Energy Ductility

Another method for assessment of ductility is energy based where the ratio between the amount of inelastic energy that would be absorbed by the system up to failure, E_{in}, to the total energy absorbed by the system, E_{total}. The inelastic energy is computed as the difference between the total energy, E_{total}, and the elastic energy, E_{el}, that would be released by the system if it were to be unloaded just before failure. The elastic energy, E_{el}, is computed as the area of the triangles relating to each specimen in

Figure 44 and Figure 45 assuming that the unloading branch is parallel to the initial elastic stiffness of the specimen. The energy-based ductility measure was used by Grace et al. and Okeil in studying FRP-strengthened concrete structures (Grace et al. 1998; Okeil 2003). Table 12 summarizes the energy ductility percentages for the tested specimens. Both deformation and energy ductility methods show that the stiffened beam is not perfectly brittle. GFRP stiffened Square and Rectangular panels have the energy ductility values of 55 and 65% respectively which are although smaller than the same ductility values of unstiffened ones, still showing more ductile behavior rather than brittle, which corresponds to an energy ductility equal to 55.37 and 65.77 for square panel and rectangular panel specimens respectively.

5.2 Parametric Study Results

5.2.1 Predicting Shear Capacity Using Code Equations

Table 11 and Table 12 represent the predicted nominal shear capacities for the modeled rectangular and square panel specimens according to AASHTO. By applying the introduced equations to the modeled square panel specimens, it can be seen that steel and GFRP stiffening shift the buckling mode of the specimens in all cases. For the slenderest web thickness, 1/8”, the unstiffened web falls within the range of Eq. (3c) and the elastic buckling mode is predicted.

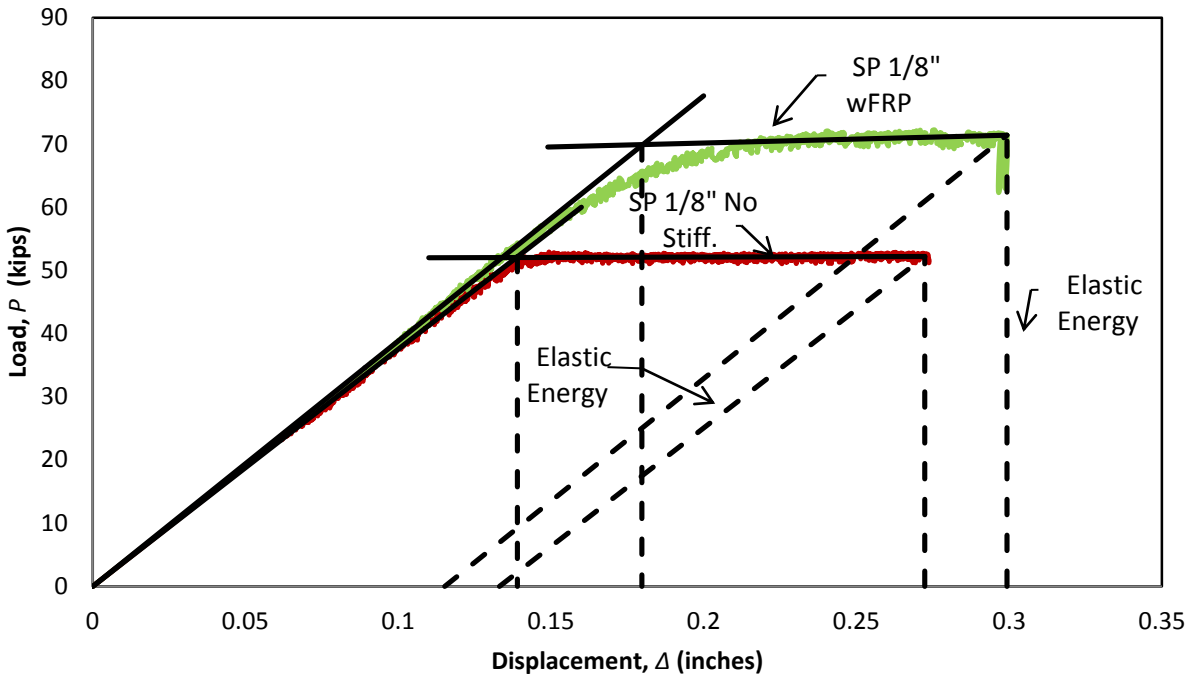

Figure 44– Energy Ductility for the Tested Square Panel Specimens

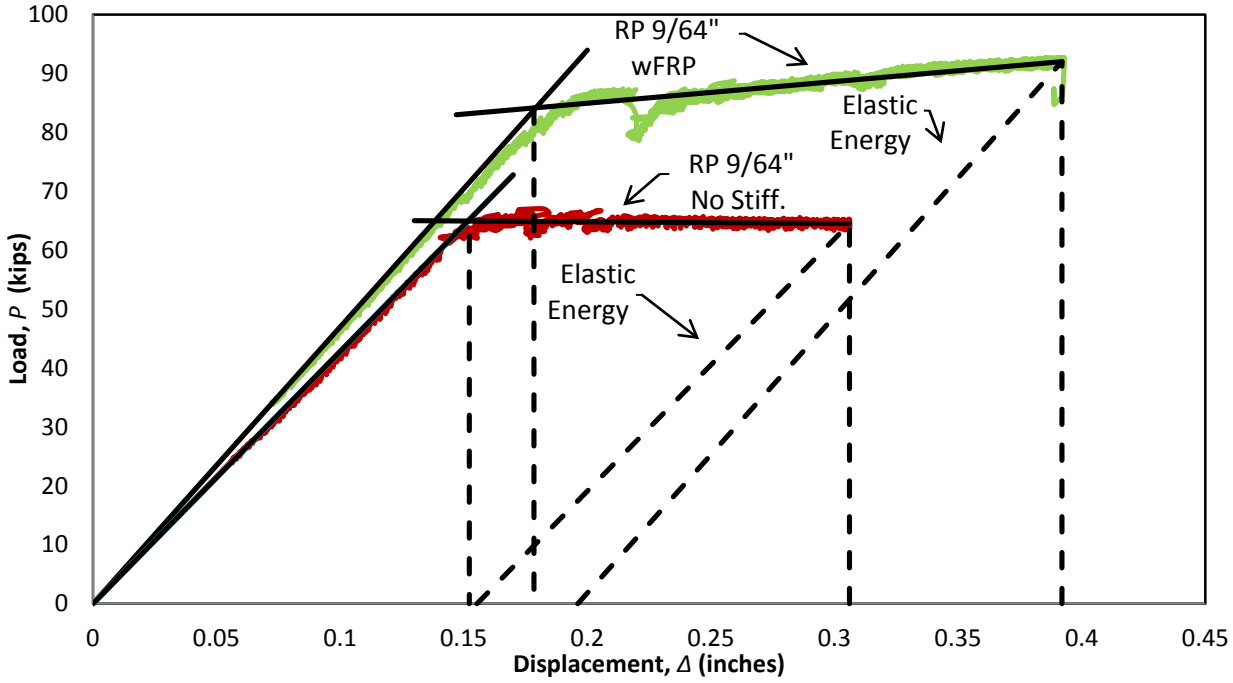

Figure 45– Energy Ductility for the Tested Square Panel Specimens

Table 10 – Summary of energy ductility percentages for tested beams

Energy Ductility		
Web Thickness (in)	Stiffening	Tested Specimens Energy Ductility (%)
SP 1/8"	No Stiff.	65.58
	GFRP 3" Flange	55.37
RP 9/64"	No Stiff.	67.49
	GFRP 6" Flange	65.77

However, stiffening the web with proposed stiffening models with either steel or GFRP stiffeners doubles the *C* value and makes the nominal shear value very close to the plastic shear strength. It also changes the failure mode from elastic buckling to inelastic buckling. Similar shifts in buckling mode happen for less slender web thicknesses. The predicted buckling modes alter from elastic to plastic and from inelastic to plastic in thicknesses of 5/32" and 3/16" respectively, which leads to higher nominal shear capacities. For the thicker web thicknesses, the value of *C* is equal to 1 based on Eq. (3.1) and the plastic shear strength becomes equal to the nominal shear value and failure mode is shear yielding. Similar results were achieved in rectangular panel cases. According to Table 6, for the thinnest web thickness, 1/8", the buckling mode is elastic. Even strengthening the web with steel stiffener still keeps the buckling mode in elastic zone. However, stiffening the web with GFRP stiffener dramatically shifts the failure mode to shear yielding and increases the value of C=0.32 to C=1.00. Therefore, full plastic capacity of shear strength of 63.80 kip, which was achieved experimentally, can be used instead of the very lower shear capacity of 20.11 kip computed based on C= 0.32. In the second case, web thickness of 5/32", steel stiffening the web changes the elastic buckling mode to inelastic mode. However, GFRP steel stiffening mode alters the elastic buckling mode to a pure shear yielding. In all modeled cases, the more the thickness becomes, the less the necessity of GFRP stiffening becomes.

5.2.2 Deformation Ductility

Based on the introduced deformation ductility method earlier, Table 13 and Table 14 list the ductility estimates for the FRP stiffened square and rectangular panel specimens, respectively.

The deformation ductility for the FRP stiffened beam increases from 3.3 to 9.10 and from 2.24 to 3.99 in square panel and rectangular panel specimens, respectively, as the web thickness ascends. Moreover, the deformed ductility of the GFRP stiffened beams increase as the thickness of the web increases. On the other hand, for unstiffened and steel stiffened specimens, increase in web thickness results in decrease in deformed ductility. The values of deformed ductility of GFRP stiffened specimens are close to the ductility of unstiffened and steel stiffened specimens. In fact, it can be said that the proposed technique of stiffening improves the performance of buckling-prone steel members by delaying the initiation of buckling, and consequently changing the failure mode.

5.3 Development of Design Coefficient

The design coefficients were established using the relative ratios of shear capacities of the beams with various range of FRP stiffener widths, steel stiffener, and without stiffener based on the analyzed FE models. In this section an attempt is made to assess the efficiency of SBS strengthened beams with the goal of deriving a coefficient that can be used in the design of such a complex system.

The approach relies on analytical results from the parametric study where the ratio between the SBS strengthened beams, V_{SBS}, and the steel stiffened beams, V_{SS}, indicates the efficiency of the SBS technique. Values greater than 1.0 mean that SBS is more efficient than

traditional steel stiffeners. Conversely, values less than 1.0 mean that welded steel stiffeners are more efficient than SBS.

Table 11 - Nominal shear resistance of the modeled SP specimens according to AASHTO

Nominal Shear Resistance of the SP Specimens								
Web Thickness (in)	Stiffening	$\frac{D}{t_w}$	$1.12\sqrt{\frac{Ek}{F_{yw}}}$	$1.40\sqrt{\frac{Ek}{F_{yw}}}$	C	V_p (kip)	V_n (kip)	Failure Mode
1/8"	No Stiff.	60	93	117	0.43	63	27	Elastic
	SS	160	147	184	0.92	63	58	Inelastic
	GFRP 3" Flange	60	147	184	0.92	63	58	Inelastic
	GFRP 4" Flange	60	147	184	0.92	63	58	Inelastic
	GFRP 6" Flange	60	147	184	0.92	63	58	Inelastic
	GFRP 8" Flange	160	147	184	0.92	63	58	Inelastic
5/32"	No Stiff.	128	93	117	0.67	79	53	Elastic
	SS	128	147	184	1.00	79	79	Shear Yielding
	GFRP 3" Flange	128	147	184	1.00	79	79	Shear Yielding
	GFRP 4" Flange	128	147	184	1.00	79	79	Shear Yielding
	GFRP 6" Flange	128	147	184	1.00	79	79	Shear Yielding
	GFRP 8" Flange	128	147	184	1.00	79	79	Shear Yielding
3/16"	No Stiff.	106	93	117	0.97	95	92	Inelastic
	SS	106	147	184	1.00	95	95	Shear Yielding
	GFRP 3" Flange	106	147	184	1.00	95	95	Shear Yielding
	GFRP 4" Flange	106	147	184	1.00	95	95	Shear Yielding
	GFRP 6" Flange	106	147	184	1.00	95	95	Shear Yielding
	GFRP 8" Flange	106	147	184	1.00	95	95	Shear Yielding
1/4"	No Stiff.	80	93	117	1.00	127	127	Shear Yielding
	SS	80	147	184	1.00	127	127	Shear Yielding
	GFRP 3" Flange	80	147	184	1.00	127	127	Shear Yielding
	GFRP 4" Flange	80	147	184	1.00	127	127	Shear Yielding
	GFRP 6" Flange	80	147.20	184	1.00	127	127	Shear Yielding
	GFRP 8" Flange	80	147.20	184	1.00	127	127	Shear Yielding
5/16"	No Stiff.	64	93.80	117	1.00	159	159	Shear Yielding
	SS	64	147.20	184	1.00	159	159	Shear Yielding
	GFRP 3" Flange	64	147.20	184	1.00	159	159	Shear Yielding
	GFRP 4" Flange	64	147.20	184	1.00	159	159	Shear Yielding
	GFRP 6" Flange	64	147.20	184	1.00	159	159	Shear Yielding
	GFRP 8" Flange	64	147.20	184	1.00	159	159	Shear Yielding

Table 12 - Nominal shear resistance of the modeled RP specimens according to AASHTO

Nominal Shear Resistance of the Modeled RP Specimens								
Web Thickness (in)	Stiffening	$\frac{D}{t_w}$	$1.12\sqrt{\frac{Ek}{F_{yw}}}$	$1.40\sqrt{\frac{Ek}{F_{yw}}}$	C	V_p (kip)	V_n (kip)	Failure Mode
1/8"	No Stiff.	160	80	100	0.32	63	20	Elastic
	SS	160	110	138	0.60	63	38	Elastic
	GFRP 6" Flange	160	110	138	0.60	63	38	Elastic
5/32"	No Stiff.	128	80	100	0.49	79	39	Elastic
	SS	128	110	138	0.94	79	74	Inelastic
	GFRP 6" Flange	128	110	138	0.94	79	74	Inelastic
3/16"	No Stiff.	106	80	100	0.71	95	67	Elastic
	SS	106	110	138	1.00	95	95	Shear Yielding
	GFRP 6" Flange	106	110	138	1.00	95	95	Shear Yielding
1/4"	No Stiff.	80	80	100	1.00	127	127	Shear Yielding
	SS	80	110	138	1.00	127	127	Shear Yielding
	GFRP 6" Flange	80	110	138	1.00	127	127	Shear Yielding
5/16"	No Stiff.	64	80	100	1.00	159	159	Shear Yielding
	SS	64	110	138	1.00	159	159	Shear Yielding
	GFRP 6" Flange	64	110	138	1.00	159	159	Shear Yielding

Table 13 – Square panel specimens' deformation ductility*

SP Deformation Ductility						
Web Thickness (in)	Unstiffened Beams	GFRP Stiffened Beams				Steel Stiffened Beams
		3" Flange	4" Flange	6" Flange	8" Flange	
1/8"	22.22	3.03	4.09	4.27	5.18	12.05
5/32"	16.67	4.38	4.93	5.62	6.16	11.11
3/16"	13.70	5.54	5.90	6.75	7.47	10.75
1/4"	9.09	7.80	8.00	4.90	7.40	9.13
5/16"	6.10	9.10	5.60	5.51	7.93	7.19

*The final deformation of the beams under load was considered 1 inch.

Table 15 and Table 16 list the analytical results for all cases considered in the parametric study. In addition to the shear capacities for the unstiffened beams, $V_{NoStiff}$, SBS-strengthened beams, V_{SBS}, and the steel stiffened beams, V_{SS}, the ratios of the shear strengths using both strengthening technique, V_{SBS}/V_{SS}, are also listed in the tables.

Table 14 - Rectangular panel specimens' deformation ductility*

RP Deformation Ductility			
Web Thickness (in)	Unstiffened Beams	GFRP Stiffened Beams 6" Flange	Steel Stiffened Beams
1/8"	14.29	2.24	11.11
5/32"	12.05	2.32	9.90
3/16"	9.09	2.11	8.55
1/4"	8.00	3.22	4.83
5/16"	5.93	3.99	4.57

*The final deformation of the beams under load was considered 1 inch.

According to the values in Table 15 and Table 16, it can be seen that the V_{SBS}/V_{SS} ratio, which can be thought of as an efficiency coefficient, is on average equal to 1.04 for square panel steel beams, and 1.03 for rectangular ones. Interestingly, the standard deviation for both cases is low, which is a testament to the consistency of the developed model. As can be seen in Figure 46, a rising trend is shown for beams with low slendernesses, which quickly stabilizes for a value slightly greater than unity. Similar conclusion can be drawn from Figure 47 for rectangular panel specimens.

It should be noted that even through SBS appears to be as efficient, if not more efficient than the traditional steel stiffeners, caution is warranted before using current code. First, the parametric study is listed in scope and more runs will be needed before a universal efficiency coefficient can be established. Second, SBS reduces the ductility of the steel member and therefore more attention should be given to the design by increasing the reliability index; i.e., reducing the probability of failure. This effort requires an intensive investigation of the structural reliability of the new system to statically calibrate the design coefficient.

Table 15 – Design coefficients for square panel specimens

Web Thickness (in)	$V_{NoStiff.}$	V_{SBS}				V_{SS}	Coefficients (6" Flange)		
	Unstiffened Beams	GFRP Stiffened Beams 3" Flange	4" Flange	6" Flange	8" Flange	Steel Stiffened Beams	$V_{SBS}/V_{NoStiff.}$	$V_{SS}/V_{NoStiff.}$	V_{SBS}/V_{SS}
1/8"	47	65	67	70	75	65	1.51	1.39	1.08
5/32"	65	84	85	89	93	81	1.36	1.24	1.10
3/16"	89	102	103	106	110	99	1.20	1.12	1.07
1/4"	128	136	137	139	142	134	1.09	1.05	1.04
5/16"	162	172	167	172	174	173	1.07	1.16	0.92
								Ave.	1.04
								STDV	0.073

Table 16 – Design coefficients for rectangular panel specimens

Web Thickness (in)	$V_{NoStiff.}$	V_{SBS}	V_{SS}	Coefficients		
	Unstiffened Beams	GFRP Stiffened Beam 6" Flange	Steel Stiffened Beams	$V_{SBS}/V_{NoStiff.}$	$V_{SS}/V_{NoStiff.}$	V_{SBS}/V_{SS}
1/8"	44.69	60.92	57.48	1.36	1.29	1.06
5/32"	63.45	79.38	76.59	1.25	1.21	1.04
3/16"	80.23	97.70	93.10	1.22	1.16	1.05
1/4"	125.62	132.95	130.31	1.06	1.04	1.02
5/16"	159.54	164.42	163.32	1.03	1.02	1.01
					Ave.	1.03
					STDV	0.021

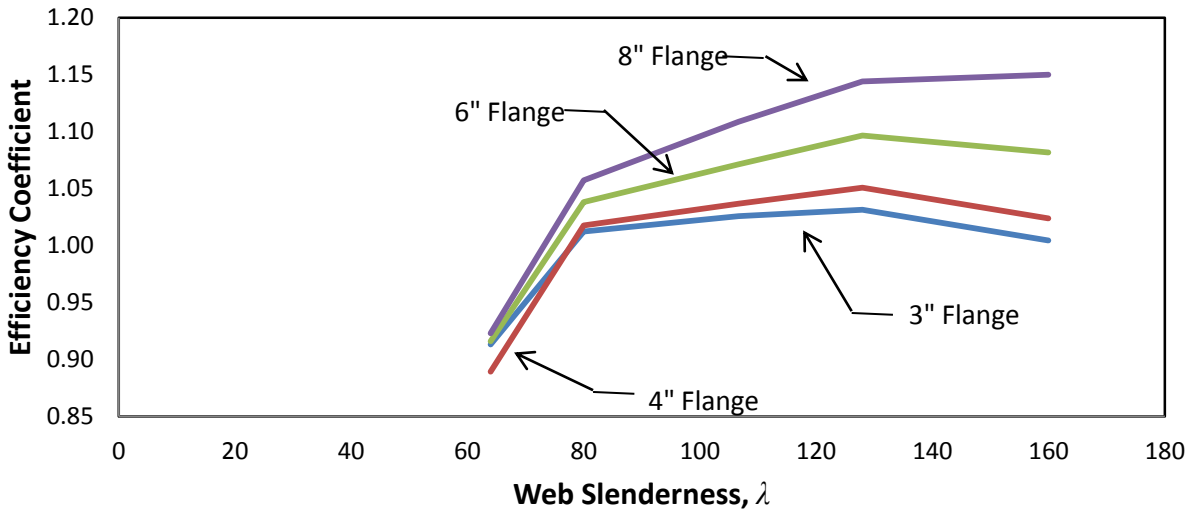

Figure 46 – Efficiency coefficient - web slenderness plot for square panel specimens

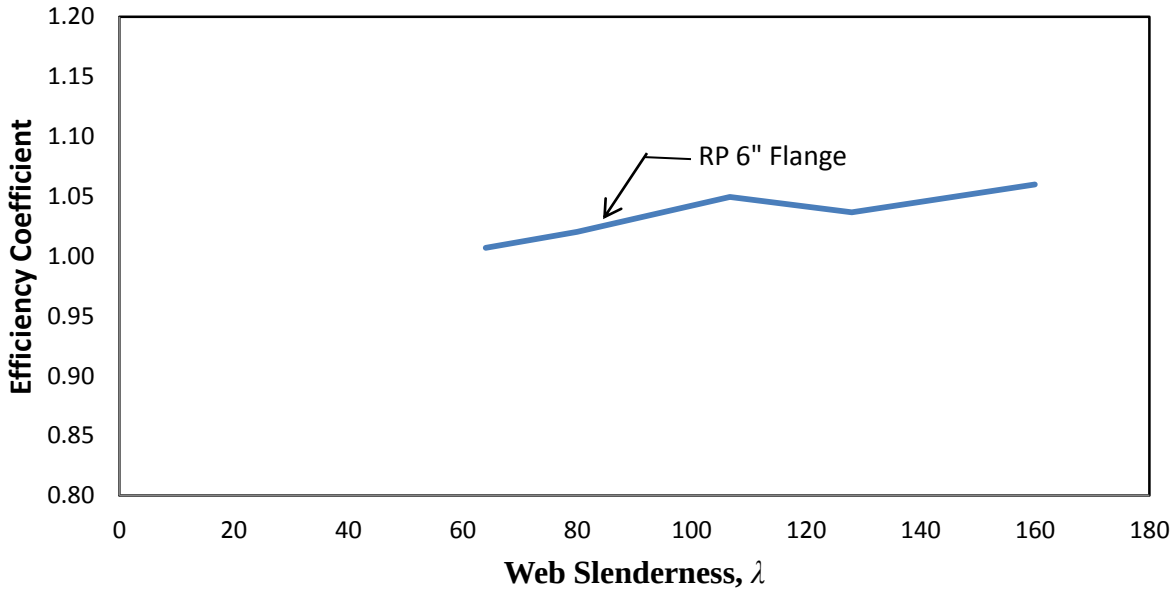

Figure 47– Efficiency coefficient – web slenderness plot for rectangular panel specimen

CHAPTER 6: SUMMARY AND CONCLUSIONS

6.1 Summary

In this study, a new strengthening method developed at Louisiana State University and referred to as Strengthening-By-Stiffening (SBS), was further investigated experimentally and numerically. SBS increases the structural strength by bonding GFRP sections to thin-walled steel plates, which has proven to be a practical technique for inhibiting local buckling in shear-controlled steel beams. This technique relies on the out-of-plane stiffness of pultruded composite sections as opposed to the in-plane strength of thin composites that is often reported in the literature. The proposed technique does not necessarily require High Modulus Fiber Reinforced Polymers (HM FRPs) and high end adhesive materials which are usually costly and uneconomic to be considered in structural and bridge engineering projects. Conversely, the use of FRP materials with low modulus material properties in optimized orientation and optimal contact area on the thin-walled steel plates can improve the stiffness of the section considerably.

The main three parameters considered in design of the tests in this study were (1) panel geometry, square panel or rectangular panel, (2) web thickness, and (3) contact area between FRP pultruded sections and bare steel web. A total of thirty Finite Element (FE) models were created in ANSYS for a parametric study of the attributes affecting SBS behavior. Five web thicknesses equal to 1/8”, 5/32”, 3/16”, 1/4”, and 5/16” were chosen for square panel and rectangular panel specimens. Also, unstiffened as well as stiffened cases were analyzed to demonstrate the difference in behavior as a result of introducing SBS to a deficient beam. Furthermore, additional cases with steel stiffeners were analyzed to compare the difference in stiffening effects and development of a design coefficient for the new SBS system.

6.2 Conclusions

According to the parametric study, it was concluded that using T-shaped GFRP stiffeners with different flange widths can result in ultimate load increase in the range of 6% to 66% for square panel beams and 3% to 36% for rectangular panel specimens. On the other hand, using steel stiffener results in ultimate load increase percentages of 16% to 47% and 2% to 28% for square panel beams and rectangular ones respectively, which are relatively smaller than GFRP strengthening ultimate load increase percentages. Moreover, it was concluded that the behavior of the SBS beams was not brittle albeit less ductile than the unstiffened or steel stiffened beams, which is common with most FRP strengthening techniques.

Four specimens were tested in the LSU Structures Lab to validate the analytical model used in parametric cases. The specimens were grouped in two main groups, namely, Group A and Group B. In Group A, an unsitffened square panel specimen and a GFRP stiffened square panel specimen were built with nominal web thickness of 1/8", while an unsitffened rectangular panel specimen and a GFRP stiffened rectangular panel specimen with nominal web thickness of 9/64" were in Group B. Similar results to parametric study were observed for the tested specimens. The increase of ultimate shear load increase 39% and 25% for square panel specimens and rectangular panel specimens respectively.

The main objective of this study was to establish a coefficient for the efficiency of FRP stiffeners, which is lacking in the current code provisions, as compared to steel stiffeners. This coefficient can be multiplied by the capacity of steel stiffened structures using existing code provisions to obtain the capacity of an FRP stiffened member using a SBS design approach. Based on the results, the derived coefficients were found to be equal to 1.04 for square panel cases, and 1.03 for rectangular panel cases which shows that it is possible to estimate the shear

using existing equations. Interestingly, the standard deviation for both cases is low, which is a testament to the consistency of the developed model. The research is still at an early stage and further exploration is necessary both in analytical and experimental research in order to study various factors that may affect the performance of FRP strengthened thin-walled sections.

6.3 Recommendations for Future Research

In order to develop comprehensive code provisions to estimate the capacity of members strengthened with FRP materials similar to available code provisions for steel stiffeners and other traditional techniques, it is of a great importance to expand the parameters in analyses and tests on FRP strengthening techniques. In this study, limited but optimized parameters of steel properties and geometry including different web thicknesses and panel lengths for the beams, and different bond areas of FRP stiffeners were taken into consideration based on the results of recent experiments.

The following recommendations may be considered for the future analytical and experimental studies on the introduced strengthening technique;

1. Different types of epoxy can be used as adhesive materials which may result in a stronger bond between the stiffener and the steel beam's web since in all cases the mode of failure was observed to be debonding of the GFRP stiffener. Selection of the FRP type and adhesive alternatives may be based on the analytical modeling of the specimens using material properties of them in the literature or the manufacturers' datasheets. Furthermore, the thickness of the adhesive layer needs to be investigated.
2. Different ratios between out-of-plane geometry of the stiffener and the bare steel web may be considered for future analyses.

3. Alternate failure modes after the shear buckling may be investigated, e.g., lateral torsional buckling, or local buckling of the compression flange.

4. Feasibility of using the introduced strengthening method in site or on industrial scale is also needed in preparation for field applications.

5. Efficiency of FRP stiffening in different environmental conditions, especially a harsh one, is also needed to address actual field conditions.

6. The effect of cyclic loads on SBS strengthening has still not been investigated, which is important to understanding the fatigue behavior using FRP materials.

7. Maintenance and application of FRP stiffening especially in large projects may be a lot cheaper compared to traditional strengthening techniques although the initial cost is a little higher. Therefore, a Life Cycle Cost (LCC) analysis is needed for the introduced FRP strengthening technique and compared to the traditional strengthening methods.

REFERENCES

AASHTO (2004). *LRFD bridge design specifications*. AASHTO, Washington, D.C.

Abushaggur, M., and El Damatty, A. (2003). "Testing of steel sections retrofitted using FRP sheets." *Annual conference of the Canadian society for civil engineering*,CD-ROM.

Accord, N. B., and Earls, C. J. (2006). "Use of fiber-reinforced polymer composite elements to enhance structural steel member ductility," *Journal of composites for construction*, Vol. 10, No. 4, pp. 337-344.

ACI Committee 440 (1996). *State-of-the-art report on fiber reinforced plastic (FRP) reinforcement for concrete structures. ACI 440R-96*. American Concrete Institute, Farmington Hills, MI.

ACI Committee 440 (2002). *Guide for the design and construction of externally bonded FRP systems for strengthening concrete structures. ACI 440.2R-02*. American Concrete Institute, Farmington Hills, MI.

ACI Committee 440 (2003). *Guide for the design and construction of concrete reinforced with FRP bars. ACI 440.1R-03*. American Concrete Institute, Farmington Hills, MI.

AISC (2001). *Manual of steel construction—load and resistance factor design*. AISC, Chicago.

Alsayed, S. H., Al-Salloum, Y. A., and Almusallam, H. (2000). "Fibre-reinforced polymer repair materials some facts." *Proceedings of the ICE - civil engineering*,138 pp. 131-134.

ASTM Standard E 8 (2008). *Standard test methods for tension testing of metallic materials*. ASTM International, West Conshohocken, PA.

Benmokrane, B., and Rahman, H. (1998). "Durability of fiber reinforced polymer (FRP) composites for construction." University Of Sherbrook Canada.

Broussard, G. (2010). "Parametric investigation of frp stiffened steel girder webs." Master's Report.

Chiew, S. P., Yu, Y., and Lee, C. K. (2011). "Bond failure of steel beams strengthened with FRP laminates – Part 1: Model development," *Composites Part B: Engineering*, Vol. 42, No. 5, pp. 1114-1121.

CSA (2002). *Design and construction of building components with fibre-reinforced polymers. S806-02*. Canadian Standards Association, Rexdale, Ontario.

El-Tawil, S., and Ekiz, E. (2009). "Inhibiting steel brace buckling using carbon fiber-reinforced polymers: Large-scale tests," *Journal of structural engineering, American society of civil engineers*, Vol. 135, No. 5, pp. 530-538.

Estrada, I., Real, E., and Mirambell, E. (2007). "General behaviour and effect of rigid and non-rigid end post in stainless steel plate girders loaded in shear. Part I: Experimental study," *Journal of constructional steel research*, Vol. 63, No. 7, pp. 970-984.

Fawzia, S., Zhao, X. L., Al-Mahaidi, R., and Rizkalla, S. (2005). "Bond characteristics between cfrp and steel plates in double strap joints," *International journal of advanced steel construction*, Hong Kong institute of steel construction, Vol. 1, No. 2, pp. 17-27.

FYFE CO., LLC (2008) TYFO®S Epoxy, "http://www.fyfeco.com/products/epoxies.html", date accessed =6-13-2008

Grace, N. F., Soliman, A. K., Abdel-Sayed, G., and Saleh, K. R. (1998). "BEHAVIOR and ductility of simple and continuous FRP reinforced beams," *Journal of composites for construction*, Vol. 2, No. 4, pp. 186-194.

Harries, K. A., Peck, A. J., and Abraham, E. J. (2009). "Enhancing stability of structural steel sections using FRP," *Thin-walled structures*, Vol. 47, No. 10, pp. 1092-1101.

Hassan, T., and Rizkalla, S. (2002). "Flexural strengthening of prestressed bridge slabs with FRP systems," *PCI Journal*, Vol. 47, No. 1, pp. 76-93.

Khalifa, A., Gold, W. J., Nanni, A., and Aziz, A. M. I. (1998). "Contribution of externally bonded FRP to shear capacity of rc flexural members," *Journal of composites for construction*, ASCE, Vol. 2, No. 4, pp. 195-202.

Lenwari, A., Thepchatri, T., and Albrecht, P. (2006). "Debonding strength of steel beams strengthened with CFRP plates," *JOURNAL of composites for construction*, ASCE, Vol. 10, No. 1, pp. 69-78.

Liu, X., Silva, P. F., and Nanni, A. (2001). "Rehabilitation of steel bridge members with FRP composite materials." *CCC2001, Composites in construction*, pp. 613-617.

MOAVENI, S., (1999). Finite Element analysis: Theory and application with ANSYS. Upper Saddle River.

Moy, S. S. J. (2001). *FRP composites: Life extension and strengthening of metallic structures: ICE design and practice guide*. Thomas Telford.

Nanni, A. (1993). "Flexural behavior and design of rc members using FRP reinforcement," *Journal of structural engineering*, ASCE, Vol. 119, No. 11, pp. 3344-3359.

Nanni, A. (1995). "Concrete repair with externally bonded FRP reinforcement," *Concrete International*, Vol. 17, No. 6, pp. 22-26.

Okeil, A. M. (2003). "Serviceability and ductility of PSC girders strengthened in flexure using CFRP laminates." *ASCE/ SEI structures congress and exposition: Engineering smarter*, *ASCE*, pp. 1215-1220.

Okeil, A. M. (2010). "Strengthening-by-stiffening: a novel FRP technique for thin-walled steel beams." *Proceedings of the international symposium on Life-Cycle performance of highway bridges and structures*, Changsha, China.

Okeil, A. M., Bingol, Y., and Chorkey, M. (2010). "Stiffening thin-walled structures using pultruded FRP sections." *FHWA bridge engineering conference: Highways for life and accelerated bridge construction*, Orlando, Fl.

Okeil, A. M., Bingol, Y., and Ferdous, M. R. (2009a). "A novel technique for stiffening steel structures." Louisiana department of transportation and development.

Okeil, A. M., Bingol, Y., and Ferdous, M. R. (2009b). "Novel technique for inhibiting buckling of thin-walled steel structures using pultruded Glass FRP sections," *Journal of composites for construction*, Vol. 13, No. 6, pp. 547-557.

Okeil, A. M., and Broussard, G. (2012). "Efficiency of inhibiting local buckling using pultruded FRP sections." *91st annual meeting of the transportation research board*, Washington, D.C..

Okeil, A. M., Broussard, G., and Ferdous, M. R. (2012). "Effect of bond area on strengthening efficiency of FRP-stiffened thin-walled steel beams." *Proceedings of the 3rd international structural specialty conference*, Edmonton, Alberta, Canada.

Saadatmanesh, H., and Ehsani, M. (1998). *Second international conference on composites in infrastructure*, ICCI,1 and 2 pp. 1506.

Sayed-Ahmed, E. Y. (2004). "Strengthening of thin-walled steel I-section beams using CFRP strips." *4th advanced composites for bridges and structures*, Calgary, Canada.

Schnerch, D., Stanford, K., Sumner, E. A., and Rizkalla, S. (2004). "Strengthening steel structures and bridges with high-modulus carbon fiber-reinforced polymers – resin selection and scaled monopole behavior," *Transportation Research Record*, No. 1892, pp. 237-245.

Shaat, A., and Fam, A. (2006). "Axial loading tests on short and long hollow structural steel columns retrofitted using carbon fibre reinforced polymers," *Canadian journal of civil engineering*, Vol. 33, No. 4, pp. 458-470.

Shaat, A., Schnerch, D., Fam, A., and Rizkalla, S. (2004). "Retrofit of steel structures using fiber-reinforced polymers (FRP): State-of-the-art." *Transportation Research Board (TRB) annual meeting*,CD-ROM (04-4063).

Stickler, P. B. (2002). " Composite materials for commercial transport − issues and future research directions." *Proceedings of the asc, 17th annual technical conference*, West Lafayette, IN.

Strongwell Corporation (2008). EXTREN® Series 500, "http://www.strongwell.com/products/pultruded_prod/struc_shapes/index.shtml", date accessed = 6-13-2008.

Tavakkolizadeh, M. (2003). "Fatigue strength of steel girders strengthened with carbon fiber reinforced polymer patch," *J. struct. eng.*, ASCE, Vol. 129, No. 2, pp. 186.

Tavakkolizadeh, M., and Saadatmanesh, H. (2003). "Strengthening of steel-concrete composite girders using carbon fiber reinforced polymers sheets," *JOURNAL of structural engineering*, ASCE, Vol. 129, No. 1, pp. 30-40.

Teng J. G., Chen J. F., Smith S. T., and Lam L. (2002). "FRP-strengthened RC beams. II: Assessment of debonding strength models," *Engineering structures*, Vol. 24, No. 4, pp. 397-417.

Vatovec, M., Kelley, P. L., Brainerd, M. L., and Kivela, J. B. (2002). "Post strengthening of steel members with CFRP." *47th international sampe symposium and exhibition, soc. for the advancement of material and process engineering*,47 pp. 941-954.

Zhao, X. L., and Zhang, L. (2007). "State-of-the-art review on FRP strengthened steel structures," *Engineering structures*, Vol. 29, No. 8, pp. 1808-1823.

Zhao, X. L., and Al-Mahaidi, R. (2009). "Web buckling of lightsteel beams strengthened with CFRP subjected to end-bearing forces," *Thin-walled structures*, Vol. 47, No. 10, pp. 1029-1036.

VITA

Hamed BabaizadehRoshanfekr was born in February 1987 in Rasht, Iran. He received his secondary and high school education from NODET (National Organization for Development of Exceptional Talents) in Rasht, Iran. Hamed graduated with his bachelor's degree from Amirkabir University of Technology in civil engineering. During his Undergraduate studies, he worked at several construction and consulting companies before he moved to the United States for continuing his education. He got admitted for the master's program in structural engineering in the Department of Civil and Environmental Engineering at Louisiana State University in August 2011. He has been working as a graduate research assistant under supervision of Dr. Ayman Okeil and is a candidate for degree of Master of Science in Civil Engineering to be awarded in December 2012. His main areas of interests are structural rehabilitation and strengthening and bridge engineering.